Fracture Theory and Its Seismological Applications

Renata Dmowska and James R. Rice
Division of Applied Sciences and Department of Earth and Planetary Sciences, Harvard University, Cambridge, MA 02138, USA

Published in ***Continuum Theories in Solid Earth Physics***,
Vol. 3 of the series *Physics and Evolution of the Earth's Interior*;
edited by Roman Teisseyre, Elsevier and Polish Scientific Publishers,
1986, pages 187-255

3. Fracture Theory and Its Seismological Applications

3.1 INTRODUCTION

Fracture phenomena pose significant geophysical problems over a vast range of size scales. These encompass the atomistic and microstructural scales of interest for an understanding of cataclastic rock deformation and friction in the manner of materials science, the laboratory scale at which study of "macroscopic" crack growth and friction phenomena is usually attempted, and, finally, the field scale which may range from mining rockbursts to large crustal earthquakes extending over hundreds of kilometers. In this review we emphasize the study of fracture through methods of continuum mechanics and discuss applications to pre-seismic and dynamic earthquake rupturing.

The presentation is organized around theoretical models of the fracture process that envision rupture to occur along a planar zone of displacement discontinuity within a surrounding continuum, usually taken to be elastic. The "ruptured" portion, which we may call the crack, may be subject either to boundary conditions of a fixed stress drop, in which case some fracture energy must be ascribed to processes occurring at the crack tip, or it may be subject to boundary conditions which are themselves a constitutive relation between local stress and relative displacement across the crack. In the latter case, the constitutive relations must generally exhibit a reduction of strength with rapidly imposed displacement. In more elaborate but more realistic versions they may also exhibit a dependence of strength, at least for shear cracks, on slip rate and surface state, where the state itself evolves with ongoing slip in a manner that is consistent with weaking in rapidly imposed slip and with restrengthening in stationary or near-stationary contact. While the surroundings of the crack zone are normally taken to be elastic, as mentioned, some progress has been made with more complicated rheologies, such as general linear viscoelastic, non-linearly viscous Maxwellian, rate-insensitive elastic-plastic, and fluid-infiltrated poro-elastic. Research on the first three of these has been extensive in technologically-oriented fracture mechanics; probably, their wider examination in the earthquake context would be productive, although we do not discuss the topics here.

Other theoretical models of the fracture process examine a non-elastically deforming mass and seek to determine conditions under which it becomes unstable. This instability may occur dynamically, i.e. by lack of a continuing quasi-static solution to boundary conditions of slowly imposed stress or displacement. It may alternatively, or additionally, be in the form of a concentration of subsequent deformation increments into a narrow zone or shear band, as a result of what would be a bifurcation in a uniformly deformed system. Ideally, one might like to combine concepts and to imagine a complete fracture model in which inelastic deformation occurs in some region at a crack tip, and in which this deformation locally reaches conditions for concentration of deformation into a narrow zone which joins onto the crack and ultimately becomes a prolongation of the crack itself. At present there seems to be no complete and mechanically self-consistent analysis of a fracture process along these lines, although various *ad-hoc* models have been attempted to address initiation of cracking from an inelastically deforming region.

In comparing the fracture models around which we organize this review to reality, it is perhaps important to remember that fracture processes are strongly sensitive to heterogeneities. For example, what might be described at the laboratory scale as stable inelastic compressive deformation of a confined brittle rock specimen may involve, at the grain scale, a series of unstable tensile cracking and frictional slip events. Further, these give readily detected acoustic emissions. Similarly, in application of fracture models to the much larger scale of earthquakes, it is important to remember that local instabilities may be occurring over a range of size scales while the overall processes of, say, slip along a fault or stressing of some region may be stable when judged at an appropriately large size scale. Thus, what is described as stable, quasi-static advance of a crack-like zone of slippage over the size scale of large crustal earthquakes may, at a smaller size scale, involve dynamic instabilities in the form of background seismicity or perhaps foreshocks to a coming instability at the large crustal scale. Obviously, the local dynamic instabilities may occur over a range of magnitudes, some of which may involve sizes of too large a scale to be considered "microscopic" by comparison to the large crustal scale examined.

Among other sources, the material which follows in this chapter draws extensively on a review by Dmowska (1983) on crack dynamics and its seismological applications, and on portions relating to fracture modelling in geological materials in an article by Rice (1980) on the mechanics of earthquake rupture. These references and their extensive bibliographies, to some extent updated here, may be consulted for a fuller treatment.

3.2 ELASTIC-BRITTLE CRACK MECHANICS

By an "elastic-brittle" crack model, we shall understand a model in which material outside the crack remains ideally elastic and in which there is an abrupt drop in stress σ_{2j} on the plane of the crack (taken as $x_2 = 0$) as the cracked region is entered (see Fig. 3.2.1). In the case of tensile cracks (mode I, possibly in combination with II and/or III) the stresses σ_{2j} ($j = 1, 2, 3$) drop to zero on the crack plane (or to a value consistent with the pressure of some crack-filling fluid). For shear cracks (modes II and/or III), which are of interest for earthquake processes, the stress σ_{22} and displacement u_2 are continuous across the crack, whereas the shears σ_{21},

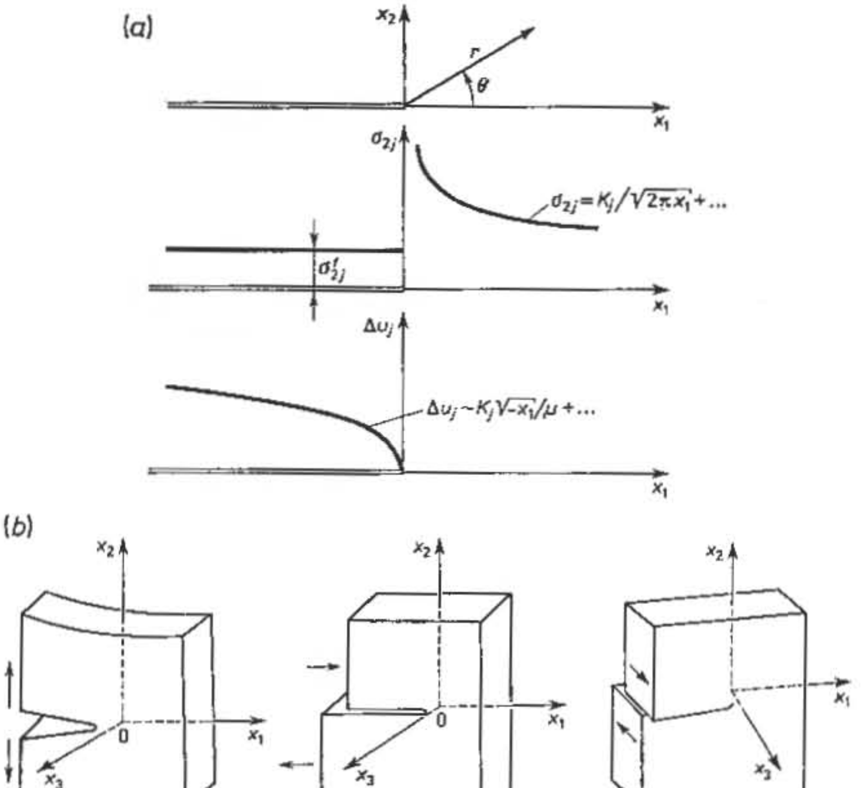

Fig. 3.2.1. Elastic crack model. (*a*) Coordinates at tip, with crack plane $x_2 = 0$ and crack front tangent to x_3 axis; stress σ_{2j}; displacement gap Δu_j. (*b*) Three modes; I is tensile opening, II is in-plane shear, III is anti-plane shear.

σ_{23} are assumed to drop abruptly to constant or slowly varying frictional values σ_{21}^f, σ_{23}^f on the crack surface, there being associated discontinuities in u_1, u_3. The abrupt drop of resisting stress on such a crack plane, embedded within an otherwise elastic solid, leads to singular stress and strain fields at the crack tip. Hence, the actual flow of energy to inelastic processes near the tip of an advancing rupture, leading to breakdown of strength, is represented within the elastic-brittle crack model by the elastic energy G that is released per unit area of new crack surface as the singular crack tip stress and strain field advances through the material. That is, in the model the entire rupture process is confined to an arc (crack tip) of singularity surrounding the (crack) surface of previously ruptured material; the material outside the crack has its undisturbed elastic properties. This elastic-brittle crack model, however unrealistic in detail, seems to provide an adequate approximation of many seismological problems (e.g. static and dynamic models of earthquake rupture, described as one planar crack and/or its development). Other models of cracks are also used, allowing the rupture process to occur in an annular zone, rather than an arc, surrounding the crack surface. This group of models, considered in Section 3.4, gives an explicit, if oversimplified, representation of the breakdown process in shear, in terms of a reduction from some high peak strength σ^p to the residual frictional strength σ^f within a zone of strength degradation at the crack tip.

3.2.1 Static crack tip stress fields; stress intensity factors

In elastic-brittle crack models the strain field in general is highly concentrated at the crack front, which is the site of a strain singularity, while the strain ε_{33} and all displacement derivatives $\partial u_j/\partial x_3$ (where here x_3 has been chosen in a direction that is locally tangent to the crack front at the point considered; Fig. 3.2.1) necessarily remain bounded and small due to constraint of surrounding material. Consider the implications of this remark in terms of the governing equations of an elastic field in terms of displacements. These equations follow within the usual assumptions of linear and isotropic elasticity from

$$\begin{aligned} &\partial\sigma_{ij}/\partial x_i = \varrho\partial^2 u_j/\partial t^2 \\ &\sigma_{ij} = \lambda\delta_{ij}\partial u_h/\partial x_h + \mu(\partial u_i/\partial x_j + \partial u_j/\partial x_i) \end{aligned} \tag{3.2.1}$$

(λ, μ are the Lamé elastic moduli, ϱ is the density), and hence have the Navier form

$$(\lambda+\mu)\left[\frac{\partial}{\partial x_1},\frac{\partial}{\partial x_2},\frac{\partial}{\partial x_3}\right]\left(\frac{\partial u_1}{\partial u_1}+\frac{\partial u_2}{\partial x_2}+\frac{\partial u_3}{\partial x_3}\right)$$
$$+\mu\left(\frac{\partial^2}{\partial x_1^2}+\frac{\partial^2}{\partial x_2^2}+\frac{\partial^2}{\partial x_3^2}\right)[u_1,u_2,u_3] = \varrho\frac{\partial^2}{\partial t^2}[u_1,u_2,u_3] \qquad (3.2.2)$$

Evidently, for asymptotic solution for the crack tip singular field from these equations, all terms involving $\partial/\partial x_3$ can be deleted on grounds that they either are bounded or are one order less singular than the remaining terms with spatial derivatives. Also, in the case of a stationary or only slowly advancing crack, the inertia terms $\varrho\partial^2 u_i/\partial t^2$ may be disregarded near the tip by comparison to the spatial derivative terms (see Section 3.2.4 to follow for inclusion of dynamic effects in rapid crack growth), and hence the near-tip singular field satisfies the statical equations

$$(\lambda+\mu)\left[\frac{\partial}{\partial x_1},\frac{\partial}{\partial x_2},0\right]\left(\frac{\partial u_1}{\partial x_1}+\frac{\partial u_2}{\partial x_2}\right)+\mu\left(\frac{\partial^2}{\partial x_1^2}+\frac{\partial^2}{\partial x_2^2}\right)$$
$$\times[u_1,u_2,u_3] = [0,0,0] \qquad (3.2.3)$$

These equations, valid asymptotically for three-dimensional crack problems, are the same equations which govern two-dimensional elastic plane strain (for u_1 and u_2) and anti-plane strain (for u_3) fields. Hence their solutions may be written through well-known methods of two-dimensional elasticity (Muskhelishvili, 1953) in terms of analytic functions $\varphi(\zeta)$, $\psi(\zeta)$, $\omega(\zeta)$ of the complex variable $\zeta = x_1+\mathrm{i}x_2$

$$\begin{aligned}2\mu(u_1+\mathrm{i}u_2) &= (3-4\nu)\varphi(\zeta)-\zeta\overline{\varphi'(\zeta)}-\overline{\psi(\zeta)}\\ 2\mathrm{i}\mu u_3 &= \omega(\zeta)-\overline{\omega(\zeta)}\end{aligned} \qquad (3.2.4)$$

where i is the unit imaginary number, ν is Poisson's ratio, and the overbar denotes complex conjugation. The resulting stresses are

$$\begin{aligned}\sigma_{11}+\sigma_{22} &= \sigma_{33}/\nu = 2\varphi'(\zeta)+2\overline{\varphi'(\zeta)}\\ \sigma_{22}-\sigma_{11}+2\mathrm{i}\sigma_{12} &= 2\bar{\zeta}\varphi''(\zeta)+2\psi'(\zeta)\\ \sigma_{32}+\mathrm{i}\sigma_{31} &= \omega'(\zeta)\end{aligned} \qquad (3.2.5)$$

Following the method of Rice (1968a), based on analytic function theory, the only singular solution of these equations consistent with bounded tractions on the crack faces and giving finite displacements is

$$\begin{aligned}\varphi(\zeta) &= (K_2-\mathrm{i}K_1)(\zeta/2\pi)^{1/2}\\ \psi(\zeta) &= (K_2+3\mathrm{i}K_1)(\zeta/8\pi)^{1/2}\\ \omega(\zeta) &= 2K_3(\zeta/2\pi)^{1/2}\end{aligned} \qquad (3.2.6)$$

where K_1, K_2, K_3 are real quantities chosen to coincide with standard definitions of Irwin's crack tip stress intensity factors (e.g. Paris and Sih, 1965). Here, however, the K's have been given subscripts such that K_j corresponds to a crack displacement discontinuity Δu_j, where

$$\Delta u_j = u_j(x_1, 0^+, x_3) - u_j(x_1, 0^-, x_3) = u_j|_{\theta=\pi} - u_j|_{\theta=-\pi}$$

the latter with reference to Fig. 3.2.1, and induces concentrated stress σ_{2j} along the $x_1 x_3$ plane ahead of the crack tip. Thus K_2 corresponds to mode I, K_1 to mode II, and K_3 to mode III; i.e. with the usual method of denoting modes by Roman numericals, Fig. 3.2.1,

$$[K_{\mathrm{II}}, K_{\mathrm{I}}, K_{\mathrm{III}}] = [K_1, K_2, K_3]$$

In particular, the stress distribution acting on the plane $\theta = 0$ directly adjacent to the crack front is

$$\sigma_{2j}|_{\theta=0} = K_j/(2\pi r)^{1/2} + \sigma^{\mathrm{f}}_{2j} + O(r^{1/2}) \tag{3.2.7}$$

where the $r^{-1/2}$ singular term is calculated from the equations for the analytic functions above, where the bounded term σ^{f}_{2j} is the limiting value of the traction acting on the crack surfaces $\theta = \pm\pi$ as $r \to 0$, and where the additional terms, denoted by the order symbol, vanish at the crack tip. Similarly, the displacement discontinuity along the crack is

$$\Delta u_j = [(1-\nu)K_j + \nu\delta_{j3}K_3](8r/\pi)^{1/2}/\mu + O(r^{3/2}), \tag{3.2.8}$$

where ν is the Poisson ratio $\lambda/2(\lambda+\mu)$.

The full angular distribution of tbe $r^{-1/2}$ singular stress field, and resulting $r^{1/2}$ displacement field, may be determined by substitution of the solutions for φ, ψ, ω above into the equations for σ_{ij} and u_i in terms of tbese functions. The results are given in many sources (e.g. Paris and Sih, 1965; Rice, 1968a; Lawn and Wilshaw, 1975, which contains plots of various components against θ) and are not reproduced here.

Many solutions to elastostatic crack problems have been developed, and extensive tabulations of solutions are given by Paris and Sib (1965), Tada *et al.* (1973), and in a series of books edited by Sih (1973, 1975). Certain features of solutions are now cited for some simple problems of planar cracks, on $x_2 = 0$, wbich are well isolated from boundaries of the crack-containing body. Suppose the loadings on the body are such that a stress field $\sigma^0_{ij}(x_1, x_2, x_3)$ would exist in tbe body if the crack surfaces were constrained to have zero relative displacement, but that a stress σ^{f}_{2j} is actually transmitted across the crack plane in the natural cracked state. The stress drops $\Delta\sigma_j$ (variahle with positions x_1, x_3 along the crack plane in general) are defined by

$$\Delta\sigma_j(x_1, x_3) = \sigma^0_{2j}(x_1, 0, x_3) - \sigma^{\mathrm{f}}_{2j}(x_1, x_3) \tag{3.2.9}$$

Now, for a "tunnel" crack, extending indefinitely in the $\pm x_3$ directions and with edges at $x_1 = \pm a$, which sustains *uniform* stress drops, the relative displacements along the crack surfaces are given by

$$\Delta u_j = 2[(1-\nu)\Delta\sigma_j + \nu\delta_{j3}\Delta\sigma_3](a^2-x_1^2)^{1/2}/\mu \tag{3.2.10}$$

whereas the stress acting on the crack plane outside the crack ($|x_1| > a$) is given by

$$\sigma_{2j}(x_1, 0, x_3) = \sigma_{2j}^0(x_1, 0, x_3) + \Delta\sigma_j[|x_1|(x_1^2-a^2)^{-1/2}-1] \tag{3.2.11}$$

By comparison of either of these results to the previous expressions for near tip fields in terms of stress intensity factors, it is evident that

$$K_j = \Delta\sigma_j(\pi a)^{1/2} \tag{3.2.12}$$

Another problem which has a simple but useful solution is that of the circular crack, with front at $x_1^2+x_3^2 = a^2$ along $x_2 = 0$, subject also to a uniform stress drop. In this case the relative displacements of the crack faces are

$$\Delta u_j = 4(1-\nu)(2\Delta\sigma_j - \nu\delta_{j2}\Delta\sigma_2)(a^2-x_1^2-x_3^2)^{1/2}/(2-\nu)\pi\mu \tag{3.2.13}$$

and the stress intensity factors at the point $x_1 = a$, $x_2 = x_3 = 0$ along the crack front are given by

$$[K_1, K_2, K_3] = [2\Delta\sigma_1/(2-\nu), \Delta\sigma_2, 2(1-\nu)\Delta\sigma_3/(2-\nu)](4a/\pi)^{1/2} \tag{3.2.14}$$

(this corrects eq. (5.13) of Rice (1980), where the factor $(1-\nu)$ for K_3 is missing).

The results given thus far could be derived from the result of Eshelby (1957): A homogeneous ellipsoidal inclusion, embedded in a homogeneous elastic body subject to remotely uniform stress, undergoes a state of uniform strain. By specialization to an inclusion of vanishing moduli, and then letting one principal axis of the ellipsoid approach zero so that the ellipsoid degenerates to a crack, we conclude that for uniform stress drops $\Delta\sigma_j$ on an elliptical crack occupying the region

$$x_1^2/a^2 + x_3^2/c^2 \leqslant 1 \quad \text{on } x_2 = 0$$

the relative displacements must be given by

$$\Delta u_i = A_{ij}\Delta\sigma_j(1-x_1^2/a^2-x_3^2/c^2)^{1/2}/\mu \tag{3.2.15}$$

where the matrix A_{ij} of coefficients, necessarily diagonal for the given choice of axes, is homogeneous of degree one in a and c, and dependent also on the Poisson ratio ν. Values of the A_{ij} can be obtained either by specialization of the results by Eshelby (1957), e.g. Budiansky and O'Connell (1976), Budiansky and Rice (1978), or by an energy-based argument stemming from work of Irwin (1962) and given by Hoenig (1978). Presuming $a > c$,

$$\begin{aligned}
A_{11} &= 2(1-\nu)ck^2\{(k^2-\nu)E(k)+\nu(1-k^2)K(k)\}^{-1} \\
A_{22} &= 2(1-\nu)c/E(k) \\
A_{33} &= 2(1-\nu)ck^2\{[k^2+\nu(1-k^2)]E(k)-\nu(1-k^2)K(k)\}^{-1} \\
A_{12} &= A_{21} = A_{23} = A_{32} = A_{31} = A_{13} = 0 \qquad (3.2.16)
\end{aligned}$$

where $k^2 = 1-c^2/a^2$, and where $K(k)$ and $E(k)$ are the complete elliptic integrals of first and second kind, respectively.

As an application of the foregoing solution for Δu_j under uniform stress drops, we apply an elegant theorem by Madariaga (1979; see also Rice, 1980) based on elastic reciprocity to state the following: Let the elliptical crack considered above be subjected to an arbitrary, *non*-uniform distribution of stress drop, $\Delta\sigma_j(x_1, x_3)$. Then the components of the moment tensor M_{ij} of the relative displacement distribution are given by

$$\begin{aligned}
M_{ij} &\equiv \mu \int_S (\delta_{i2}\Delta u_j + \delta_{j2}\Delta u_i)\mathrm{d}x_1\,\mathrm{d}x_3 \\
&= (\delta_{i2}A_{kj}+\delta_{j2}A_{ki}) \int_S \Delta\sigma_k(x_1, x_3)(1-x_1^2/a^2-x_3^2/c^2)^{1/2}\mathrm{d}x_1\,\mathrm{d}x_3 \qquad (3.2.17)
\end{aligned}$$

where S denotes the surface of the elliptical crack and δ_{i2} enters as the i component of unit normal to this surface. Thus, for example, if only the stress drop component $\Delta\sigma_1$ is non-zero, the non-vanishing components of M_{ij} are

$$\begin{aligned}
M_{12} &= M_{21} = \mu \int_S \Delta u_1\,\mathrm{d}S \\
&= A_{11} \int_S \Delta\sigma_1(x_1, x_3)(1-x_1^2/a^2-x_3^2/c^2)^{1/2}\mathrm{d}x_1\,\mathrm{d}x_3 \qquad (3.2.18)
\end{aligned}$$

and for the special case of a *uniform* stress drop this reduces to

$$\begin{aligned}
&M_{12} = M_{21} = (2\pi/3)acA_{11}\Delta\sigma_1 \qquad (3.2.19) \\
&[= 16(1-\nu)a^3\Delta\sigma_1/3(2-\nu) \quad \text{when } c = a]
\end{aligned}$$

The result above for M_{12} is used extensively to estimate $\Delta\sigma_1$ (which should perhaps be called the *nominal* shear stress drop) from seismically observed moments when some independent means (aftershock zone size, surface breakage, geodetic changes, corner frequency of spectrum) is available to estimate the size of the rupture. The nominal stress drops estimated thereby for large crustal earthquakes generally fall in the range of 1 to 10 MPa, with values in the 3 to 6 MPa range being most representative (Kanamori, 1977).

However, it should be understood that only very smooth rupture propagation on a uniform fault surface would be approximated successfully by a uniform stress drop model, and, in reality, it should be expected that local stress drops fluctuate highly along the rupture surface and such a model would give only the (weighted, e.g. as in eq. (3.2.18)) average value of a real stress drop (see Aki, 1979; Madariaga, 1979; Rice, 1980; Rudnicki and Kanamori, 1981). It might be also noted here that many large shallow earthquakes represent "multiple events" rather than the development of one planar crack, and thus more sophisticated crack models should be used to approximate the real source process. For example, rupture models with barriers along a single fault surface, Section 3.3, show that propagation may be slowed or stopped completely at some barriers on the way, perhaps starting again on a disconnected fault surface in the latter case.

It is expected that uniform stress drops models might provide better approximations for deeper earthquakes than for shallow ones, because events deeper than approximately 40 km seem to exhibit relatively smooth spectra, possibly reflecting a greater uniformity of stress and material conditions at such depths.

3.2.2 Integral representations for elastic-brittle cracks and integral equations

Returning to the case of the tunnel crack, another solution (which will be useful for analysis of slip weakening models in Section 3.4) is that which corresponds to a stress drop $\Delta\sigma_j$ which is not uniform but, rather, which varies with x_1 over the width $-a < x_1 < +a$ of the crack; i.e. $\Delta\sigma_j = \Delta\sigma_j(x_1)$. Further, suppose that the region $x_1 < -a$, $x_2 = 0$ (i.e. the portion of the crack plane lying to the left of the crack itself) is cut and given the uniform relative displacements $\Delta u_j = D_j$, where D_1, D_2, D_3 are given constants. These constants represent the net Burgers vector of displacements within the crack. This problem is formulated conveniently by singular integral equations (Muskhelishvili, 1953a, b; Bilby and Eshelby, 1968). Thus, observing that $-\mathrm{d}\Delta u_1(x_1)/\mathrm{d}x_1$ can be regarded as the density of continuously distributed line dislocations along the plane $x_2 = 0$, and recalling that a line dislocation at $x_1 = \xi$ creates stresses elsewhere on the x_1 axis proportional to $1/(x_1-\xi)$, one has the integral representation of the alteration of stress field σ_{2j} on $x_2 = 0$ in terms of relative displacements

$$-\frac{\mu}{2\pi(1-\nu)}\int_{-a}^{a}\frac{1}{x_1-\xi}\frac{\mathrm{d}}{\mathrm{d}\xi}[\Delta u_j(\xi)-\nu\delta_{j3}\Delta u_3(\xi)]\mathrm{d}\xi$$

Here the integral is to be interpreted in principal value sense if $|x_1| < a$, and the relative displacement Δu_j must be consistent with the stress drop distribution, such that

$$\Delta\sigma_j(x_1) = \frac{\mu}{2\pi(1-\nu)}\int_{-a}^{+a}\frac{1}{x_1-\xi}\frac{\mathrm{d}}{\mathrm{d}\xi}[\Delta u_j(\xi)-\nu\delta_{j3}\Delta u_3(\xi)]\mathrm{d}\xi$$

$$\text{for} \quad -a < x_1 < +a \tag{3.2.20}$$

and must, further, be consistent with the given net dislocations D_j within the crack

$$\int_{-a}^{+a}\frac{\mathrm{d}}{\mathrm{d}\xi}\Delta u_j(\xi)\mathrm{d}\xi = -D_j \tag{3.2.21}$$

Regarding the stress drop distribution as given, the second to last equation is a singular integral equation with Cauchy kernel, and the supplementary condition given by the last equation enables its unique solution

$$\frac{\mathrm{d}}{\mathrm{d}x}\Delta u_j(x) = -\frac{2}{\pi\mu(a^2-x^2)^{1/2}}\int_{-a}^{+a}\frac{(a^2-\xi^2)^{1/2}}{x-\xi}[(1-\nu)\Delta\sigma_j(\xi)$$

$$+\nu\delta_{j3}\Delta\sigma_3(\xi)]\mathrm{d}\xi-\frac{D_j}{\pi(a^2-x^2)^{1/2}}, \quad -a < x(\equiv x_1) < +a \tag{3.2.22}$$

The associated stress intensity factors may be determined by comparing the above result, near $x_1 = \pm a$, to the asymptotic expression for Δu_j near a crack tip (eq. (3.2.8)). Hence, at the respective crack tips $\pm a$,

$$K_j = \frac{1}{(\pi a)^{1/2}}\int_{-a}^{+a}\left(\frac{a\pm x}{a\mp x}\right)^{1/2}\Delta\sigma_j(x)\mathrm{d}x\pm\frac{\mu(D_j-\nu\delta_{j3}D_3)}{2(1-\nu)(\pi a)^{1/2}} \tag{3.2.23}$$

Several comments are in order on possible generalizations of the solution method just outlined. First, consistently with the elastic-brittle crack model, it has been assumed that the stress drop $\Delta\sigma_j(=\sigma^0_{2j}-\sigma^f_{2j})$ is some given quantity. More elaborate crack models would, however, relate σ^f_{2j} (and hence $\Delta\sigma_j$ also) to the current relative displacements Δu_k or perhaps, more generally, to their recent time history in the manner of a functional relation (see Section 3.4). In that case the integral eq. (3.2.20) remains valid but now the Δu's appear on the left also, in a generally non-linear manner. Solutions must then be developed numerically as in work by Cleary (1976), Stuart (1979a, b) and Stuart and Mavko (1979), some results of which will be discussed subsequently in connection with slip-weakening models. The basic formulation outlined above must also be modified for cracks that are near to external boundaries, e.g. as in the Dmowska and Kostrov (1973) analysis of a dip-slip fault. In this case the basic $1/(x_1-\xi)$ dependence of the stress field of a line dislocation in eq. (3.2.20) is modified, at least for two-dimensional elastic fields, to

$$[1/(x_1-\xi)]+h(x_1, \xi)$$

where $h(x_1, \xi)$ is non-singular within the body considered. Hence the integral eq. (3.2.20) contains a kernel with a regular term in addition to the Cauchy singular term. Efficient numerical solution methods in terms of Tchebychev polynomials (e.g. Erdogan and Gupta, 1972) are available for this case.

Analogous integral equation procedures can be formulated for three-dimensional crack problems. For example, let $U_{kj}(\mathbf{x}, \boldsymbol{\xi})$ be the elastostatic Green's function for the region considered, i.e. the k component of displacement at $\mathbf{x}$ due to a unit point force in the j direction at $\boldsymbol{\xi}$, and let c_{ijpq} be the modulus tensor $[\mathrm{d}\sigma_{ij} = c_{ijpq}\mathrm{d}(\partial u_p/\partial x_q)]$. By reciprocity, $U_{kj}(\mathbf{x}, \boldsymbol{\xi}) = U_{jk}(\boldsymbol{\xi}, \mathbf{x})$. Then by a well-known representation theorem, the change u_k in displacement field due to imposed relative displacements Δu_p along some surface S is

$$u_k(\mathbf{x}) = \int_S \frac{\partial U_{kj}(\mathbf{x}, \boldsymbol{\xi})}{\partial \xi_i} c_{ijpq}(\boldsymbol{\xi}) n_q(\boldsymbol{\xi}) \Delta u_p(\boldsymbol{\xi}) \, \mathrm{d}^2\boldsymbol{\xi} \tag{3.2.24}$$

Here, if the sides of S are labelled $+$ and $-$, then $\Delta u_p = u_p^+ - u_p^-$ and n_q is the unit normal to S pointing in the direction from $-$ to $+$. The associated stress field is given by

$$\begin{aligned} \sigma_{ij}(\mathbf{x}) &= \sigma_{ij}^0(\mathbf{x}) + c_{ijrs}(\mathbf{x})\, \partial u_r(\mathbf{x})/\partial x_s \\ &= \sigma_{ij}^0(\mathbf{x}) + \int_S c_{ijrs}(\mathbf{x}) \frac{\partial^2 U_{rn}(\mathbf{x}, \boldsymbol{\xi})}{\partial x_s \partial \xi_m} c_{mnpq}(\boldsymbol{\xi}) n_q(\boldsymbol{\xi}) \Delta u_p(\boldsymbol{\xi}) \, \mathrm{d}^2\boldsymbol{\xi} \end{aligned} \tag{3.2.25}$$

Now, consider the special case for which all external boundaries are remote for the crack surface S and for which the modulus tensor c_{ijpq} is spatially uniform. In such a case the Green's function is translationally invariant,

$$U_{rn}(\mathbf{x}, \boldsymbol{\xi}) = \hat{U}_{rn}(\mathbf{x}-\boldsymbol{\xi}) = \hat{U}_{nr}(\boldsymbol{\xi}-\mathbf{x}) \tag{3.2.26}$$

Further, assume that S lies in the plane $x_2 = 0$ so that $n_q = \delta_{q2}$, let the Greek index α range over the values 1 and 3 (i.e. over coordinates in the plane of the crack), and, following an observation by Budiansky and Rice (1979) for an analogous dynamical problem, note that by symmetry of the modulus tensor and by the equilibrium equations satisfied by the Green's function,

$$\frac{\partial}{\partial \xi_2}\left[\frac{\partial \hat{U}_{nr}(\boldsymbol{\xi}-\mathbf{x})}{\partial \xi_m} c_{mnp2}\right] + \frac{\partial}{\partial \xi_\alpha}\left[\frac{\partial \hat{U}_{nr}(\boldsymbol{\xi}-\mathbf{x})}{\partial \xi_m} c_{mnp\alpha}\right] = 0 \tag{3.2.27}$$

when $\boldsymbol{\xi} \neq \mathbf{x}$. The second derivative of the Green's function in eq. (3.2.25) can be written as $-\partial^2 U_{nr}(\boldsymbol{\xi}-\mathbf{x})/\partial \xi_s \partial \xi_m$, and the sum on the repeated index s in that equation is done first as a sum over 1 and 3 (with s represented by α) and then by adding the additional term with $s = 2$, but simplified by eq. (3.2.27) above. Thus one obtains

$$\sigma_{ij}(\mathbf{x}) = \sigma^0_{ij}(\mathbf{x}) - (c_{ijr\alpha} c_{mnp2} - c_{ijr2} c_{mnp\alpha}) \int_S \frac{\partial^2 \hat{U}_{nr}(\boldsymbol{\xi}-\mathbf{x})}{\partial \xi_\alpha \partial \xi_m} \Delta u_p(\boldsymbol{\xi}) \mathrm{d}\xi_1 \mathrm{d}\xi_3 \tag{3.2.28}$$

which can be integrated by parts to give, since Δu_p vanishes at the crack front,

$$\sigma_{ij}(\mathbf{x}) = \sigma^0_{ij}(\mathbf{x}) - (c_{ijr\alpha} c_{mnp2} - c_{ijr2} c_{mnp\alpha}) \int_S \frac{\partial \hat{U}_{nr}(\boldsymbol{\xi}-\mathbf{x})}{\partial \xi_m} \frac{\partial}{\partial \xi_\alpha} \Delta u_p(\boldsymbol{\xi}) \mathrm{d}\xi_1 \mathrm{d}\xi_3 \tag{3.2.29}$$

This last equation is the three-dimensional version of the representation given just before eq. (3.2.20) for two-dimensional elastic fields.

For elastically isotropic materials,

$$c_{ijrs} = \lambda \delta_{ij} \delta_{rs} + \mu(\delta_{ir} \delta_{js} + \delta_{is} \delta_{jr}) \tag{3.2.30}$$

and

$$\hat{U}_{nr}(\mathbf{x}) = \frac{1}{8\pi\mu(\lambda+2\mu)}\left[(\lambda+3\mu)\frac{\delta_{nr}}{|\mathbf{x}|} - (\lambda+\mu)\frac{x_n x_r}{|\mathbf{x}|^3}\right] \tag{3.2.31}$$

Thus, if we let $\mathbf{x}$ approach the plane S of the crack in eq. (3.2.29), thereby evaluating stress components $\sigma_{2j}(\mathbf{x})$ for $\mathbf{x}$ on S, and if we note that then $\sigma_{2j} = \sigma^f_{2j} = \sigma^0_{2j} - \Delta\sigma_j$, where $\Delta\sigma_j$ is the stress drop, there results after some computation the set of integral equations (see Weaver, 1977, or the low frequency limit of Budiansky and Rice, 1979, for details of the computation)

$$\Delta\sigma_2(\mathbf{x}) = -\frac{\mu(\lambda+\mu)}{2\pi(\lambda+2\mu)}\int_S \frac{R_\alpha}{R^3}\frac{\partial}{\partial\xi_\alpha}\Delta u_2(\boldsymbol{\xi})\,\mathrm{d}\xi_1\,\mathrm{d}\xi_3$$

$$\Delta\sigma_\beta(\mathbf{x}) = -\frac{\mu(\lambda+\mu)}{4\pi(\lambda+2\mu)}\int_S\left[\frac{\mu}{\lambda+\mu}\left(\frac{R_\alpha\delta_{\beta\gamma}-R_\beta\delta_{\alpha\gamma}}{R^3}\right)\right. \tag{3.2.32}$$

$$\left. +\frac{3R_\alpha R_\beta R_\gamma}{R^5}\right]\frac{\partial}{\partial\xi_\alpha}\Delta u_\gamma(\boldsymbol{\xi})\,\mathrm{d}\xi_1\,\mathrm{d}\xi_3$$

for $\mathbf{x}$ on S, where $R_\alpha = \xi_\alpha - x_\alpha$, $R = |\boldsymbol{\xi}-\mathbf{x}|$, and where Greek indices α, β and γ range over 1 and 3 only. In cases for which the stress drop is given, these are singular integral equations which can be solved numerically; an effective procedure has been developed and illustrated by Weaver (1977).

When the region considered contains boundaries or surfaces of discontinuity in elastic moduli which are not distant from the crack site, the Green's function can be written as

$$U_{rn}(\mathbf{x},\boldsymbol{\xi}) = \hat{U}_{rn}(\mathbf{x}-\boldsymbol{\xi})+H_{rn}(\mathbf{x},\boldsymbol{\xi}) \tag{3.2.33}$$

where the first term is the Green's function for an unbounded homogeneous solid with elastic properties identical to those, presumed locally uniform, in the region where the crack occurs and the second, bounded term accounts for finite boundaries or other nearby discontinuities. Then it is evident that the integral expression relating stress drop $\Delta\sigma_j(\mathbf{x})$ to $\Delta u_p(\mathbf{x})$ are the same as in eqs. (3.2.32) above, except that the right-hand side of the equation for $\Delta\sigma_j(\mathbf{x})$ contains the additional term, calculated from eq. (3.2.25),

$$-\int_S c_{2jrs}c_{mnp2}\frac{\partial^2 H_{rn}(\mathbf{x},\boldsymbol{\xi})}{\partial x_s\partial\xi_m}\Delta u_p(\boldsymbol{\xi})\,\mathrm{d}\xi_1\,\mathrm{d}\xi_3$$

where the c's here are moduli in the vicinity of the crack site, and hence given for an isotropic material by eq. (3.2.30) in terms of the local λ and μ. This addition to the integral equations has a bounded kernel and should pose no special problems in numerical solution. To our knowledge, a formulation like the one outlined here has not yet been applied for three-dimensional crack problems in other than unbounded bodies. Some details of the formulation require modification when the crack surface S intersects a boundary because the transformation from eqs. (3.2.28) to (3.2.29) assumes that Δu_p vanishes on the boundary of S, and this would not be true for a surface-breaking crack. A detailed analysis of the two-dimensional (plane strain) integral equation formulation for a surface-breaking crack has been given in the paper by Dmowska and Kostrov (1973).

Another feature noted in that paper for cracks near boundaries (or other discontinuities) is the following: Slip displacements Δu_1 and/or Δu_3 alter not only the shear stresses σ_{21} and σ_{23} along the crack plane but, in general, also alter the *normal* stress σ_{22}. (Equations (3.2.32) show that this same coupling of shear displacement to normal stress does not occur for isolated cracks in homogeneous unbounded bodies). Hence, if the boundary condition on shear stress along the crack is coupled to normal stress, as will normally be the case for sliding friction, the shear stress drops $\Delta\sigma_a$ cannot be specified *a priori*. Suppose, for example, that one is concerned with slip Δu_1 along a shear crack under conditions for which the resistive shear stress σ^f_{21} is not itself prescribed but, rather, an expression of the kind $\sigma^f_{21}+\eta\sigma^f_{22}$ (where η is a friction coefficient) is prescribed along the crack surface. In this case we can regard the linear combination of stress drops

$$\Delta\sigma_1+\eta\Delta\sigma_2 \equiv (\sigma^0_{21}+\eta\sigma^0_{22})-(\sigma^f_{21}+\eta\sigma^f_{22}) \tag{3.2.34}$$

as a given function along the crack. Thus, if we write the integral relations between stress drops and relative crack surface displacements discussed above in the symbolic form

$$\Delta\sigma_j(\mathbf{x}) = L_{jk}(\mathbf{x}, \boldsymbol{\xi}) * \Delta u_k(\boldsymbol{\xi}) \tag{3.2.35}$$

the integral equation $\Delta\sigma_1 = L_{11}*\Delta u_1$ which would govern the case without normal stress effects is replaced by the equation

$$\Delta\sigma_1+\eta\Delta\sigma_2 = (L_{11}+\eta L_{21})*\Delta u_1 \tag{3.2.36}$$

for the given quantity in this case, where the coupling operation $L_{21}*$ vanishes for an unbounded homogeneous body, eq. (3.2.32), and, in a finite or non-uniform body, involves an integral operation on Δu_1 with a bounded kernel.

Analogously to the static representation of eq. (3.2.24), we have the well-known dynamical representation

$$u_k(\mathbf{x}, t) = \int_{-\infty}^{t}\int_{S(\tau)} \frac{\partial G_{kj}(\mathbf{x}, \boldsymbol{\xi}, t-\tau)}{\partial \xi_i} c_{ijpq}(\boldsymbol{\xi})\eta_q(\boldsymbol{\xi})\Delta u_p(\boldsymbol{\xi}, \tau)\mathrm{d}^2\boldsymbol{\xi}\mathrm{d}\tau \tag{3.2.37}$$

where the dynamic Green's function $G_{kj}(\mathbf{x}, \boldsymbol{\xi}, t)$ is the k component of displacement at $\mathbf{x}$, at time t, due to a unit point impulse applied in the j-direction at $\boldsymbol{\xi}$ at time 0. Here the notation $S(\tau)$ denotes the rupture surface at time τ. By calculating $\sigma_{ij}(\mathbf{x}, t)-\sigma^0_{ij}(\mathbf{x}, t) = c_{ijpq}(\mathbf{x})\partial u_p(\mathbf{x}, t)/\partial x_q$ from the above expression it is possible at least formally to develop integral relations represented symbolically by

$$\Delta\sigma_j(\mathbf{x}, t) = L_{jk}(\mathbf{x}, \boldsymbol{\xi}, t-\tau) * \Delta u_k(\boldsymbol{\xi}, \tau) \tag{3.2.38}$$

and to interpret these as governing integral equations of crack problems for which $\Delta\sigma_j$ is prescribed. Budiansky and Rice (1979) have outlined such a formulation for the case of planar cracks of fixed size subjected to time harmonic $\Delta\sigma$'s and responding in steady state with time harmonic Δu's.

However, the integral formulation of dynamic crack problems which has thus far found most use in applications is that due to Hamano (1974), developed and applied extensively by Das (1976, 1980, 1981) and Das and Aki (1977a, b). In this formulation the solution for time-dependent loading on the surface of a homogeneous elastic half-space (with boundary at, say $x_2 = 0$) is used to construct an integral representation of the form

$$\Delta u_j(\mathbf{x}, t) = 2 \int_{-\infty}^{t} \int_{-\infty}^{+\infty} \int_{-\infty}^{+\infty} \overline{G}_{jk}(\mathbf{x}-\boldsymbol{\xi}, t-\tau)\Delta\sigma_k(\boldsymbol{\xi}, \tau)\mathrm{d}\xi_1\mathrm{d}\xi_3\mathrm{d}\tau \qquad (3.2.39)$$

where $\mathbf{x}$ and $\boldsymbol{\xi}$ in this equation are field and source points, respectively, on the planes $x_2 = 0$ and $\xi_2 = 0$, and $\overline{G}_{jk}$ (which is translationally invariant for such choices of $\mathbf{x}$ and $\boldsymbol{\xi}$) is the dynamic Green's function for the elastic half-space. In this case $\Delta\sigma_1(\boldsymbol{\xi}, \tau)$, for example, is regarded as given over the region $S(\tau)$ occupied by the crack at time τ, and the condition $\Delta u_1(\mathbf{x}, t) = 0$ for $\mathbf{x}$ outside $S(t)$ converts the above representation into an integral equation for $\Delta\sigma_k(\boldsymbol{\xi}, \tau)$ at points $\boldsymbol{\xi}$ lying outside the rupture. These points extend to infinity in the ξ_1- and ξ_3-directions but, in dynamical applications, the necessity to deal numerically with an unbounded region is avoided because waves have carried displacement signals only a finite distance beyond the (typically enlarging) crack surface.

3.2.3 Energy release in crack growth; path independent integrals

Consider quasi-static growth of an elastic-brittle crack, Fig. 3.2.2, which currently occupies a surface S (with bounding contour L, denoting the crack front); we describe infinitesimal crack advance by the local length

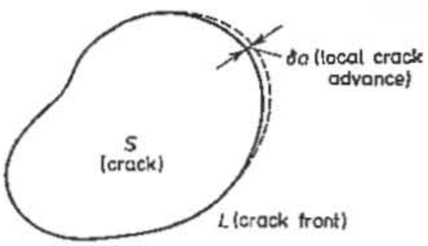

Fig. 3.2.2. A three-dimensional crack surface S; bounding contour L denotes the crack front and local advance by amount δa (variable with position along L) is shown.

of crack expansion δa measured perpendicular to the crack front at each point of L. The infinitesimal δa is a function of position along L, and it is regarded as an arbitrary non-negative function for purposes of the present discussion. A local energy release rate per unit area of crack advance, namely G, is defined at each point along L by requiring that

$$\delta W_{ext} = \delta E + \int_S n_i \sigma_{ij}^f \delta(\Delta u_j) \mathrm{d}S + \int_L G \delta a \mathrm{d}L \tag{3.2.40}$$

for arbitrary distribution along L of crack growth δa. Here the δ quantities are associated with the considered crack growth, δW_{ext} is the increment of work by applied forces (e.g. gravity) acting on the body during this growth, and E is the elastic strain energy stored in the body. The equation thus states that the excess of δW_{ext} over δE accounts for the sum of energy dissipated by work of the (frictional) resistive stresses $n_i \sigma_{ij}^f$ acting on the crack surfaces *and* by the energy flow G per unit new crack area to breakdown processes at the advancing crack front.

If the external forces are conservative, as we suppose, the difference between $(E-E^0)$ and W_{ext}, where superscript "0" denotes the "uncracked" state (precisely, the arbitrarily chosen state for which we choose to say that $\Delta u_k = 0$ on S and identify the stress field then acting in the body as σ_{ij}^0) and where W_{ext} is measured from zero at this "uncracked" state, is given by the work of quasi-statically reducing the stress acting on the crack from $n_i \sigma_{ij}^0$ to $n_i \sigma_{ij}^f$, so that the relative displacements Δu_j develop. Hence $(E-E^0) - W_{ext}$ has no dependence on the particular process by which the current crack surface S and distribution of $n_i \sigma_{ij}^f$ over it were attained, but depends only on the location of that surface and current stress distribution on it. If the crack surroundings and any displacement dependent external loadings are modelled as linear elastic, we have

$$(E-E^0) - W_{ext} = -\tfrac{1}{2} \int_S (n_i \sigma_{ij}^0 + n_i \sigma_{ij}^f) \Delta u_j \mathrm{d}S \tag{3.2.41}$$

Here the 1/2 results from linearity and the negative sign from the convention adopted previously for n_k.

Hence the equation defining G is

$$\delta \left[\tfrac{1}{2} \int_S (n_i \sigma_{ij}^0 + n_i \sigma_{ij}^f) \Delta u_j \mathrm{d}S \right] - \int_S n_i \sigma_{ij}^f \delta(\Delta u_j) \mathrm{d}S = \int_L G \delta a \mathrm{d}L \tag{3.2.42}$$

The left-hand side of this equation is phrased exclusively in terms of quantities defined on the crack surface S. Further, by introducing the stress drops $\Delta\sigma_j$ along S, defined by

$$\Delta\sigma_j = n_i \sigma_{ij}^0 - n_i \sigma_{ij}^f \tag{3.2.43}$$

and substituting for $n_i\sigma^0_{ij}$ in the above relation, we can rearrange the left side to

$$\delta\left[\int_S n_i\sigma^f_{ij}\Delta u_j+\tfrac{1}{2}\Delta\sigma_j\Delta u_j\,\mathrm{d}S\right]-\int_S n_i\sigma^f_{ij}\delta(\Delta u_j)\,\mathrm{d}S$$

$$=\int_S \delta(n_i\sigma^f_{ij})\,\Delta u_j\,\mathrm{d}S+\delta\left[\tfrac{1}{2}\int_S\Delta\sigma_j\Delta u_j\,\mathrm{d}S\right] \tag{3.2.44}$$

Noting now that σ^0_{ij} is a fixed stress distribution, the variation in resistive stress $\delta(n_i\sigma^f_{ij})$ along the crack surface during a growth increment is just the negative of variation in stress drop $\Delta\sigma_j$, and thus the equation defining G is

$$\delta\left[\tfrac{1}{2}\int_S\Delta\sigma_j\Delta u_j\,\mathrm{d}S\right]-\int_S\delta(\Delta\sigma_j)\Delta u_j\,\mathrm{d}S=\int_L G\delta a\,\mathrm{d}L \tag{3.2.45}$$

We recall from the various integral relations of the last section that, for a given elastic body, the Δu's are determined uniquely by the distribution of stress drops, $\Delta\sigma$, on any given surface S. Hence the last equation shows that G is determined, at each point along the crack front, by the position of the crack surface, S, and by the distribution of stress drops along this surface.

It is now advantageous to remember that the state which we denote by "0" can be chosen rather arbitrarily. This is the state from which we choose to measure relative displacements Δu_j along the crack (i.e. we say that $u_j = 0$ at state "0"), and the only requirement for validity of our formulae is that $n_i\sigma^0_{ij}$ be identified as the stresses acting along S in the state which we have chosen. For purposes of a certain calculation that follows, we will make the choice of "0" as the state when the crack occupies surface S, Fig. 3.2.2, just before the infinitesimal growth by δa takes place. Then Δu_j has temporary interpretation as the additional displacement of the crack surfaces during the advance δa and, indeed $\delta(\Delta u) = \Delta u$. In the circumstances, the second integral on the left in eq. (3.2.45), involving $\delta(\Delta\sigma_j)$ [$= -\delta(n_i\sigma^f_{ij})$], goes to zero faster than δa and the portion of the first integral that is carried out over all the crack surface *except* the part newly created by the advance δa likewise goes to zero faster than δa. Hence, just as in the classical calculation by Irwin (1960), the integral involving $\frac{1}{2}\Delta\sigma_j\Delta u_j$ need be carried out only over the newly generated crack surface to have the requisite accuracy to first order in δa. Further, if the growth increments δa are directed such that the crack surface is continuously curved, without abrupt kinking (i.e. discontinuity in direction of the normal $\mathbf{n}$), the near tip expression for Δu_j at the tip of a locally planar crack applies, eq. (3.2.8), so long as r is measured from the advanced crack tip. Thus, using eqs. (3.2.7) for $\Delta\sigma_j$ and (3.2.8) for Δu_j in eq. (3.2.45), which defines G along the crack front, we have (thinking now of the x_1 direction as being locally normal to L, in the direction of growth δa, and x_3 locally tangent to L, so that K_1, K_2, K_3 retain their respective mode II, I and III meanings)

$$\frac{1}{2}\int_L \int_0^{\delta a} \frac{K_j}{(2\pi x_1)^{1/2}} \frac{(1-\nu)K_j+\nu\delta_{j3}K_3}{\mu}\left[\frac{8(\delta a-x_1)}{\pi}\right]^{1/2} \mathrm{d}x_1\,\mathrm{d}L$$

$$= \int_L G\delta a\mathrm{d}L \qquad (3.2.46)$$

Here we have noted that the $\Delta\sigma_j$ appropriate for the present purposes is the $\sigma_{2j}|_{\theta=0}$ of eq. (3.2.7), given as $K_j/(2\pi x_1)^{1/2}$ plus other non-singular terms which we have not included since they make no contribution to first order in δa; similarly, consistent with the required accuracy, we have not included the alterations δK of the K's in the expression for Δu_j after growth. Thus, doing the integration on x_1,

$$\int_L \frac{1}{2\mu}\left[(1-\nu)(K_1^2+K_2^2)+K_3^2\right]\delta a\mathrm{d}L = \int_L G\delta a\mathrm{d}L \qquad (3.2.47)$$

and since this holds for arbitrary distributions of δa along L, the local G is related to the local K's by Irwin's (1960) well-known expression

$$G = \frac{1}{2\mu}\left[(1-\nu)(K_1^2+K_2^2)+K_3^2\right] \qquad (3.2.48)$$

Another perspective on the calculation of energy release rates, now not limited to the quasi-static case, is given by evaluating the flow of energy into some small tube surrounding the crack tip (Fig. 3.2.3a shows a two-dimensional cross section of such a tube, with area A and contour Γ in the x_1x_2 plane). Part of this energy flux results in changes of strain energy and of kinetic energy of material within the tube, part is dissipated against resistive forces σ_{2j}^f on the portion of crack intersected by the tube, and the remainder flows to the crack tip, thereby accounting for the G per unit area of crack advance. Since the near tip singular fields are two-dimensional in character, and since the tube is ultimately to be shrunk onto the crack tip, we can address this calculation as a locally two-dimensional calculation. Hence if $\dot{a}$ is the local speed of crack advance at the portion of crack front considered, we have

$$\int_\Gamma n_k \sigma_{kj} \dot{u}_j \mathrm{d}\Gamma = \frac{\mathrm{d}}{\mathrm{d}t} \int_A (W + \tfrac{1}{2} \varrho \dot{u}_j \dot{u}_j) \mathrm{d}A + \int_{-b}^{0-} \sigma_{2j}^f \Delta \dot{u}_j \mathrm{d}x_1 + G\dot{a} \tag{3.2.49}$$

where W is the energy density, i.e. $\delta W = \sigma_{ij} \delta(\partial u_j / \partial x_i)$. In the limit when Γ is shrunk to zero length the term involving σ_{2j}^f vanishes and, after a transformation of the integral over A and observation that for terms singular at the crack tip one may write $\partial/\partial t = -\dot{a}\partial/\partial x_1$, this becomes (see Cherepanov, 1968; Atkinson and Eshelby, 1968; Kostrov and Nikitin, 1970; Freund, 1972a, for details)

$$G = \lim_{\Gamma \to 0} \int_\Gamma \left[n_i \left(W + \frac{1}{2} \varrho \dot{a}^2 \frac{\partial u_j}{\partial x_1} \frac{\partial u_j}{\partial x_1} \right) - n_k \sigma_{kj} \frac{\partial u_j}{\partial x_1} \right] \mathrm{d}\Gamma \tag{3.2.50}$$

where the limit indicates that the contour is shrunk onto the crack tip.

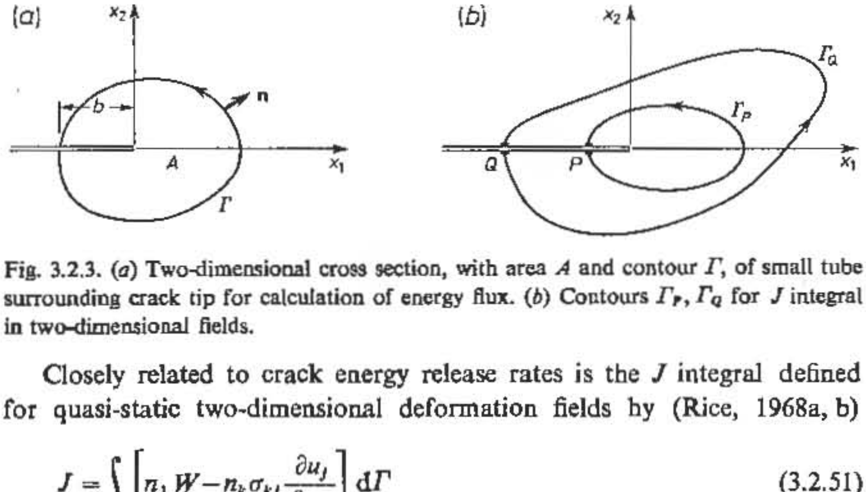

Fig. 3.2.3. (*a*) Two-dimensional cross section, with area A and contour Γ, of small tube surrounding crack tip for calculation of energy flux. (*b*) Contours Γ_P, Γ_Q for J integral in two-dimensional fields.

Closely related to crack energy release rates is the J integral defined for quasi-static two-dimensional deformation fields by (Rice, 1968a, b)

$$J = \int_\Gamma \left[n_1 W - n_k \sigma_{kj} \frac{\partial u_j}{\partial x_1} \right] \mathrm{d}\Gamma \tag{3.2.51}$$

for any path Γ that begins on the lower crack surface, encircles the tip (but no other singularities), and ends on the upper crack surface. If the crack surface is traction-free (i.e. if $\sigma_{2j}^f = 0$) this integral is independent of the path chosen. More generally, if $\sigma_{2j}^f \neq 0$, then when we evaluate the integral for two separate paths such as Γ_P and Γ_Q in Fig. 3.2.3*b*, associated with points P and Q along the crack, we have

$$J_Q - J_P + \int_{(x_1)_Q}^{(x_1)_P} \sigma_{2j}^f \frac{\partial}{\partial x_1} \Delta u_j \mathrm{d}x_1 = 0 \tag{3.2.52}$$

Here, e.g. J_Q is the value of J for any path of type Γ_Q, beginning at $[(x_1)_Q, 0^-]$ and ending at $[(x_1)_Q, 0^+]$, and J_Q has the same value for all such paths.

Evidently, if Γ_P is shrunk onto the crack tip, J_P coincides with the quasi-static version (delete $\rho\dot{a}^2$ term) of the expression in eq. (3.2.50) for G, so that for two-dimensional quasi-static crack growth,

$$G = J_Q + \int_{(x_1)_Q}^{0} \sigma_{2j}^{f} \frac{\partial}{\partial x_1} \Delta u_j \mathrm{d}x_1 \tag{3.2.53}$$

The sum of terms on the right side is, of course, independent of the point chosen as Q.

In elastic-brittle crack mechanics, the assumption is made that cracks can grow when G attains a critical value, G_c, which may itself he dependent on crack velocity. Rudnicki (1980), Rice (1980) and Wong (1982) have reviewed various attempts to infer fracture energies. For tensile cracks, standard fracture mechanics test specimens and techniques apply and $G = 3$ to $50\ \mathrm{J \cdot m^{-2}}$ is representative for mode I fracture of brittle rocks. On the other hand, direct laboratory measurements of G for shear cracks have not been possible and, only recently, such G values have been inferred from triaxial rock compression tests in stiff machines through a procedure (Rice, 1980) based on the theory of slip-weakening crack models (Section 3.4). Experiments on granite (Wong, 1982) suggest values of G for shear fracture in tbe range from approximately 5×10^3 to $5 \times 10^4\ \mathrm{J \cdot m^{-2}}$, depending on source of the granite and on confining pressure and temperature. Direct seismological inferences of G for natural earthquakes have limited reliability, but have been attempted by Husseini *et al.* (1975) and otbers (see Wong, 1982). The techniques used by Husseini *et al.* led these authors to suggest that G values in tbe range 1 to $10^4\ \mathrm{J \cdot m^{-2}}$ were appropriate for "frictional sliding" and 10^4 to $10^6\ \mathrm{J \cdot m^{-2}}$ for "fresh fracture". Choices of G necessary to make quasi-static earthquake instability predictions, based on large tectonic scale crack models, fit seismological constraints such as slip offset and nominal stress drop have in two cases (Rudnicki, 1980; Li and Rice, 1983) led to inferred values of order $4 \times 10^6\ \mathrm{J \cdot m^{-2}}$. Probably, values much in excess of tbose inferred from laboratory data, involving a single rupture plane, are due to geometric irregularities such as segmentation and *en echelon* discontinuities of natural faults (e.g. Aki, 1979; Segall and Pollard, 1980).

3.2.4 Elastic crack tip fields in dynamic crack growth

To obtain the structure of crack tip singular fields for rapidly propagating cracks, we observe that just as in the static case, derivatives involving $\partial/\partial x_3$ can be neglected by comparison to other spatially differentiated terms. Also, the accelerations $\partial^2 u_j/\partial t^2$ can be replaced by $v^2 \partial^2 u_j/\partial x_1^2$ for purposes of analysing the singularity, where v is the speed of crack advance, so that eq. (3.2.2) reduce to the following equations to be solved asymptotically:

$$\varrho(v_p^2 - v_s^2)\left[\frac{\partial}{\partial x_1}, \frac{\partial}{\partial x_2}, 0\right]\left(\frac{\partial u_1}{\partial x_1} + \frac{\partial u_2}{\partial x_2}\right)$$
$$+\varrho v_s^2\left(\frac{\partial^2}{\partial x_1^2} + \frac{\partial^2}{\partial x_2^2}\right)[u_1, u_2, u_3] = \varrho v^2 \frac{\partial^2}{\partial x_1^2}[u_1, u_2, u_3] \tag{3.2.54}$$

Here

$$v_p = [(\lambda+2\mu)/\varrho]^{1/2}, \quad v_s = (\mu/\varrho)^{1/2} \tag{3.2.55}$$

are the P- and S-wave speeds.

Following Kostrov and Nikitin (1970) one may rewrite the governing equations in terms of two displacement fields u_k^p and u_k^s, where $u_k = u_k^p + u_k^s$, $\partial u_1^p/\partial x_2 - \partial u_2^p/\partial x_1 = \partial u_1^s/\partial x_1 + \partial u_2^s/\partial x_2 = 0$, and $u_3^p = 0$. The resulting equations are then

$$\left(r_p^2 \frac{\partial^2}{\partial x_1^2} + \frac{\partial^2}{\partial x_2^2}\right)u_k^p = 0, \quad \left(r_s^2 \frac{\partial^2}{\partial x_1^2} + \frac{\partial^2}{\partial x_2^2}\right)u_k^s = 0 \tag{3.2.56}$$

where

$$r_p = (1 - v^2/v_p^2)^{1/2}, \quad r_s = (1 - v^2/v_s^2)^{1/2} \tag{3.2.57}$$

and have solutions in terms of analytic functions $U_k^p(\zeta)$, $U_k^s(\zeta)$ as

$$u_k^p = \mathrm{Re}[U_k^p(x_1 + \mathrm{i}r_p x_2)] \quad \text{with } U_2^p = \mathrm{i}r_p U_1^p,\ U_3^p = 0 \tag{3.2.58}$$

and

$$u_k^s = \mathrm{Re}\,[U_k^s(x_1 + \mathrm{i}r_s x_2)] \quad \text{with } r_s U_2^s = \mathrm{i}U_1^s \tag{3.2.59}$$

The singular solutions for these functions are then given by

$$\begin{aligned} &-\mu[(1+r_s^2)U_1^p(\zeta) + 2U_1^s(\zeta)] = K_2(\zeta/8\pi)^{1/2} \\ &(\mathrm{i}\mu/r_s)[2r_s r_p U_1^p(\zeta) + (1+r_s^2)U_1^s(\zeta)] = K_1(\zeta/8\pi)^{1/2} \\ &\mathrm{i}\mu r_s U_3^s(\zeta) = K_3(\zeta/8\pi)^{1/2} \end{aligned} \tag{3.2.60}$$

Here the notations K_1, K_2, K_3 for stress intensity factors are consistent with respective modes II, I, III as in the static case, and retain the interpretation that stresses ahead of the crack on $\theta = 0$ are given by

$$\sigma_{2j}|_{\theta=0} = K_j/(2\pi x_1)^{1/2} + \ldots \tag{3.2.61}$$

However, if the K's are chosen in this way, relating the stress σ_{2j} directly ahead of the crack to K_j in the same manner as in the static case, no matter what the crack velocity, then the relative displacements Δu_j of the crack faces at a given K_j are necessarily dependent on v. These have the form

$$\begin{aligned}\Delta u_1 &= (1-\nu)f_{II}(v)K_1(-8x_1/\pi)^{1/2}\mu + \ldots\\ \Delta u_2 &= (1-\nu)f_I(v)K_2(-8x_1/\pi)^{1/2}/\mu + \ldots\\ \Delta u_3 &= f_{III}(v)K_3(-8x_1/\pi)^{1/2}/\mu + \ldots\end{aligned} \tag{3.2.62}$$

where the functions f_I, f_{II}, f_{III} of speed v all have the property $f_k(0) = 1$, and are defined by

$$f_{II} = r_s v^2/(1-\nu)\Delta v_s^2, \quad f_I = r_p v^2/(1-\nu)\Delta v_s^2, \quad f_{III} = 1/r_s \tag{3.2.63}$$

with $\Delta = 4r_p r_s - (1+r_s^2)^2$ being the Rayleigh function. All three functions increase monotonically with crack speed and become unbounded as certain limiting speeds are approached. This limiting speed is seen to be the Rayleigh speed v_r ($\approx 0.92v_s$, for which $\Delta = 0$ if $\nu = 0.25$) for mode I and II, and the shear wave speed v_s for mode III.

The energy release rate can be calculated from eq. (3.2.50) and the result is (Kostrov and Nikitin, 1970)

$$G = \frac{1}{2\mu}\,[(1-\nu)(f_{II}K_1^2 + f_I K_2^2) + f_{III}K_3^2] \tag{3.2.64}$$

3.3 DYNAMIC CRACK MODELS OF EARTHQUAKE SOURCE PROCESSES

As suggested by the analysis of elastic wave fields generated by earthquakes, the source process represents a sudden stress drop in some local region, and the deformation process propagates through the Earth in a form similar to the dynamic development of a crack, usually along some previously existing fault surface (shallow earthquakes), and perhaps in the form of non-stationary development of a narrow deformation zone under conditions of high pressure and temperature (deep earthquakes). It is usually assumed that for the majority of earthquakes the deformation process in the source is concentrated onto only one plane, though this is not true for many cases, especially for major earthquakes, where the deformation occurs simultaneously or successively on more than one fault plane (multiple events).

Moreover, it may be assumed that the existence of tensile (open) cracks is limited to at most the highest few kilometers of the upper crust (see, e.g. Dmowska *et al.*, 1972) and that for all other regions conditions of pressure and temperature allow for shear cracks only. In order to recover information about the fracture process contained in the radiated wave field, it is necessary to assume some model describing the process in a realistic manner, although for practical reasons with the use of a small number of parameters. Because of the character of deformation in the earthquake source it seems plausible that such a process could be modelled satisfactorily with the use of dynamic crack models, in particular by propagation of a shear crack. We discuss here dynamic crack solutions and their seismological implications.

Analytical solution of the general problem of propagation of a crack for *any* given initial and boundary conditions is extremely difficult and existing solutions describe idealized cases that incorporate simplifying assumptions.

One of basic simplifying assumptions is that the developing crack moves in the same plane as at the beginning of its motion. Also, to eliminate or simplify the problem of multi-diffraction of waves emitted by the other end of developing crack, most of works are limited to cases of effectively semi-infinite or self-similar cracks. Such assumptions, stemming from reasons of mathematical tractability, limit essentially the physical utility of results obtained.

Many further dynamic crack problems have been solved with the use of numerical methods and these methods, or the combination of analytical and numerical approaches, will probably dominate in future research in this field.

3.3.1 Analytical solutions for steady and unsteady crack motion

We now review analytical solutions for dynamic crack propagation. For modelling earthquake source processes the most important class of solutions are cases with variable crack speed, but we will briefly discuss here also some problems with constant crack speed. The first such work was presented by Yoffe (1951), who emphasized the dependence of the stress distribution around the tip of a moving crack on the crack velocity. Yoffe analysed the case of a crack with finite, constant length, rupturing with constant speed at one end and healing at the other, under plane strain conditions in an infinite medium under remotely uniform stress σ_{22}^0 (hence the stress drop $\Delta\sigma_2 = \sigma_{22}^0$). In brittle materials, tensile cracks with higher speeds have a tendency to bifurcate from their initial plane, and the interpretation of this phenomenon had been sought in the distribution of stress around the tip of a moving crack. The solution showed that $\sigma_{\theta\theta}$ close to the crack tip (θ is the angle measured as in Fig. 3.2.1) had its maximum for $\theta = 0°$

only when the crack speed was less than approximately $0.6v_S$, and for higher speeds the maximum was located close to $\theta = 60°$. As shown by Yoffe, and confirmed in greater generality by analyses reviewed in Section 3.2.4, the angular dependence of the stress distribution did not depend on the crack length, so that the change in $\sigma_{\theta\theta}$ was not associated with some particular length. Yoffe (1951) suggested that her observations could be the reason for crack bifurcation at sufficiently high speed.

Subsequent analyses of crack growth in the shear modes showed (e.g. as discussed by Rice, 1980) that stresses encouraging fracture on planes other than the main crack plane become indefinitely large, compared to those associated with the main plane, as limiting crack speeds are approached. An aspect of this distortion of the stress field is discussed in Section 3.4.2 where it is suggested that such effects may be important to promoting non-planarity in rupture propagation.

The model presented by Yoffe, though very unrealistic (constant crack length), was useful in finding the geometry of the stress field around the edge of a moving crack. However other results of the model are less plausible. For example, the dynamic stress intensity factor calculated by her turned out to be independent on crack speed and equal to the analogous static stress intensity factor, eq. (3.2.12). Using the Griffith–Irwin–Orowan theory of a constant value of G necessary to maintain propagation, we see from eqs. (3.2.63) and (3.2.64) that the stress drop $\Delta\sigma_2$ necessary would diminish to zero with crack speed increasing towards v_r, the speed fo Rayleigh waves. This physically unrealistic result is associated with the steady state crack solution and an interpretation has been discussed by Rice (1968), who observes that because the dynamic stress intensity factor is here independent of crack velocity, the principal stress σ_{22} near to the tip, perpendicular to the crack plane, is finite for every finite load (or stress drop). The ratio of principal stresses σ_{22} to σ_{11} (σ_{11} acts parallel to the prospective fracture plane) diminishes to zero at the Rayleigh speed, which means that stresses σ_{11} then become unbounded; that is, each finite region around the crack tip has infinite strain and kinetic energy. Thus the above result could be interpreted in the way that if the crack is moving in a medium able to supply an enormous amount of energy near the tip, then very little load is required to maintain the crack speed.

A similar type of problem to that addressed by Yoffe was solved by Craggs (1960), who analysed semi-infinite cracks subjected to surface loads with points of application moving at the same speed as the crack. He also obtained a dynamic stress intensity factor independent of speed, and the remarks concerning the work of Yoffe apply to this case too.

Some limiting features of these analyses were removed by Broberg (1960) and Baker (1962). Broberg (1960) analysed the two-dimensional plane strain case of a self-similar tensile crack growing symmetrically from zero length with constant velocity in an infinite elastic medium. The medium had been subjected to uniform stress far from the crack hence the stress drop $\Delta\sigma_2(=\sigma_{22}^0)$ was uniform on the crack surface. The dynamic stress intensity factor depended on crack velocity in the form

$$K_2\,(\equiv K_1) = \bar{g}(v)\Delta\sigma_2\sqrt{\pi vt} \tag{3.3.1}$$

where $\bar{g}(0) = 1$ and the function $\bar{g}(v)$ diminished monotonically to zero at v_r. The motion is not consistent with a constant energy release rate, but the expression for G has the form (combine eqs. (3.3.1) and (3.2.64))

$$G = \pi(1-\nu)vtf_1(v)\,[\bar{g}(v)\Delta\sigma_2]^2/2\mu \tag{3.3.2}$$

and this expression has the property that $G \to 0$ as $v \to v_r$. Presuming that some non-zero G must be supplied for rupture, this suggests that the stress necessary to drive a crack increases without limit as $v \to v_r$. Broberg found that the crack deformed into an ellipse, just as in the static case; i.e. Δu_2 is as given by eq. (3.2.10) with $j = 2$, except that the expression on the right in eq. (3.2.10) should be multiplied by $f_1(v)\bar{g}(v)$ and a replaced by vt. Baker (1962) analysed a related problem in which, at $t = 0$, a semi-infinite tensile crack has its surfaces subjected to uniform stress drop and propagates with constant speed v; his solution is likewise consistent with $G \to 0$ as $v \to v_r$. Baker also remarked that the stress component $\sigma_{\theta\theta}$ on which Yoffe based her analysis of the bifurcation process represents the maximum principal stress only for $\theta = 0$ or $\pm\pi$, and that the maximum principal stress occurs in the range $60° < \theta < 100°$ (with direction coincident with neither θ nor r) for all crack speeds. The problem solved by Baker is equivalent to the case of spontaneous crack propagation caused by arrival of a plane homogeneous stress wave, a case treated in detail later by Achenbach and Nuismer (1970).

A problem similar to that solved by Broberg (1960), namely the problem of a self-similar circular tensile crack, developing with constant speed, was solved independently by Kostrov (1964a) and Craggs (1966), and analogous results were obtained on the limiting nature of the Rayleigh speed.

Shear crack versions of the above problems are, of course, more relevant for modelling earthquake source processes. The simplest self-similar shear crack problem which is appropriate for seismological application has been presented by Kostrov (1964b), who solved the case of a circular crack growing from zero size with constant speed in a field of shear stress and sustaining uniform stress drop. This case, although similar to that previously solved by Kostrov (1964a) for tensile cracking, is not an axially-symmetric one because of the shear stress field. Interpretation of crack propagation in terms of a limiting speed is in this case more difficult, because, depending on local conditions at the crack tip, the tip is either in plane-strain, anti-plane strain or in some mixed conditions and the limiting speeds are different for different strain situations (v_r for plane strain and v_s for anti-plane strain). This suggests that a crack model with slightly different principal radii, say elliptical with a/c proportional to $v_s/v_r \approx 1.1$ during growth, might be more realistic.

Some of the previously solved cases have been extended to anisotropic media. Broberg's solution has been generalized by Atkinson (1967) to a case of crack propagation on a material-symmetry plane of an anisotropic body. This case has been generalized further to arbitrarily situated cracks developing self-similarly in arbitrarily anisotropic bodies in works by Burridge (1968) and Burridge and Willis (1969). The latter work represents the most general problem of this class and solves for self-similar motion of an elliptical crack, starting from zero size, with uniform stress drops.

Modelling an earthquake source process as a self-similar crack propagating with constant speed seems to be a serious oversimplification of observed phenomena because, e.g. it cannot include ultimate rupture arrest. However, as remarked by Burridge (1968) and Burridge and Willis (1969), the analysis of such models could have seismological utility because first seismic motions depend only on crack motion in the early stages of crack existence. As shown by Burridge and Willis (1969), for conditions of uniform shear stress drop $\Delta\sigma_1$ the far field waves emitted by the self-similar elliptical crack have the same angular orientation as for a double couple (see, e.g. Aki and Richards, 1980) but multiplied by the factors

$$\{1-(v_1^2\gamma_1^2+v_3^2\gamma_3^2)/v_p^2\}^{-2} \quad \text{and} \quad \{1-(v_1^2\gamma_1^2+v_3^2\gamma_3^2)/v_s^2\}^{-2}$$

for P- and S-waves, respectively. Here v_1 and v_3 are the constant velocities of rupture advance along the principal x_1 and x_3 axes, respectively, of the ellipse on $x_2 = 0$ and $\boldsymbol{\gamma} = (\gamma_1, \gamma_2, \gamma_3)$ is a unit vector from the crack centre to the observation point.

Figures 3.3.1*a* and 3.3.1*b* show, in stereographic projection, the far wave fields for a double couple, and Figs. 3.3.1*c* and 3.3.1*d* show the above modifying factors, for $v_1 = 0.909v_s$ and $v_3 = 0.5v_s$. For v_1 close to the velocity of S-waves the modifying factor is highly directional and it has strong maxima in direction of $\pm x_1$ axis, which strongly deforms the S-wave pattern. The P-wave pattern appears little deformed, because v_1^2 and v_3^2

are well below v_p^2 and because the maximum of the factor modifying the P-wave field coincides with the zero of the P-wave field for a double couple. Thus the above results suggest that the S-wave field contains more discernible information about the propagation process in the earthquake source than does the P-wave field, as is evident also from general analysis of effects of propagation in the source region on far field radiation (Aki and Richards, 1980).

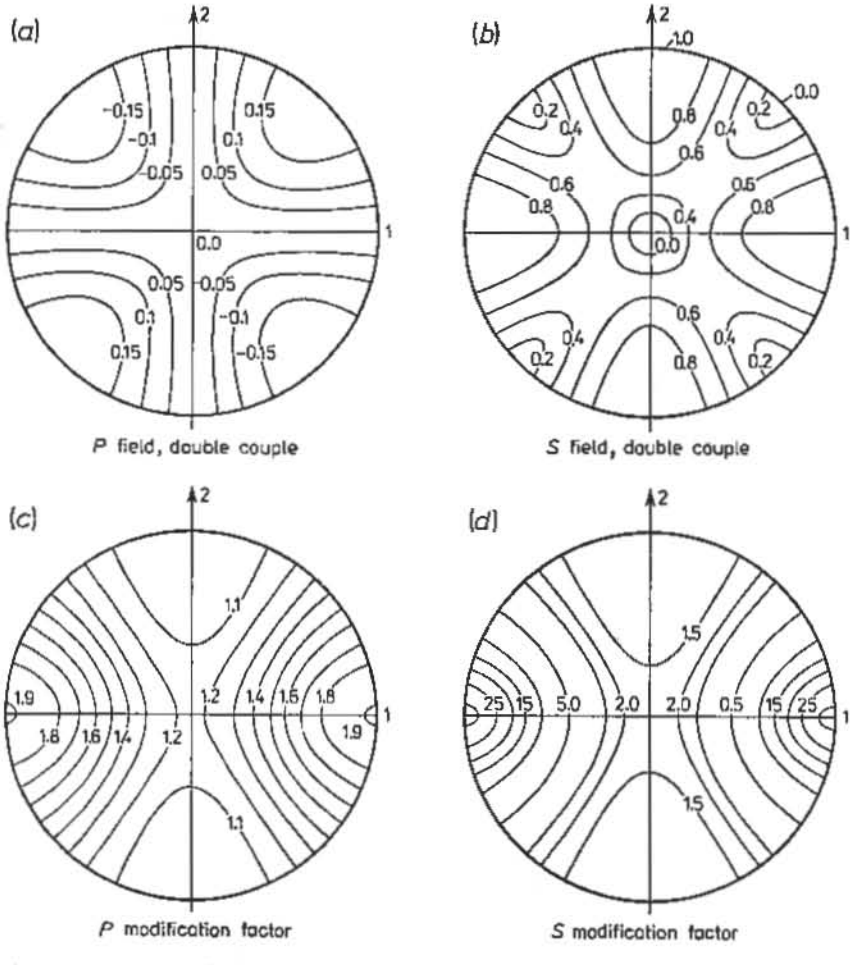

Fig. 3.3.1. (a, b) Far-field angular orientation of seismic motions, in stereographic projection, for double couple point source representation of shear stress drop $\Delta\sigma_1$ (reduction in σ_{21}) on plane $x_2 = 0$. (c, d) Modification factors to double couple field for self-similar expansion of an elliptical crack on $x_2 = 0$ with $v_1 = 0.909\, v_s$ and $v_2 = 0.5\, v_s$. From Burridge and Willis (1969).

The Craggs (1960) crack solution has been generalized by Willis (1967) to the case of a crack with a strength degradation zone close to its moving tip, and such a zone bas also been included in the Broberg crack model in works by Barenblatt *et al.* (1962) and Atkinson (1967); see Section 3.4.2 for discussion of related considerations. An interesting analytical method, similar to that used by Kostrov (1964) and allowing the reduction of many problems of self-similar propagating cracks to standard boundary problems for complex functions, has been used by Cherepanov and Afanas'ev (1974); see also Cherepanov (1979, Chapter 10). With this approach they reconstructed elegantly the solutions of Broberg and Baker as well as those to other crack problems.

To model the earthquake source processes in a realistic way one needs, however, solutions to problems of unsteady crack motion, and few have been solved analytically as yet. The first developments were for the mode III case, anti-plane shear, whicb is simpler because it is governed by a single scalar wave equation for u_3. Tbus Kostrov (1966), using analytical techniques developed for supersonic fluid flow, and independently Eshelby (1969) solved the problem of determining the stress field for arbitrary non-uniform motion and distribution of stress drop along tbe surface of a semi-infinite crack. Such provides also a short time solution for finite cracks, valid near one crack tip up to the moment when stress waves first arrive from the other tip. Two particular cases were discussed in detail by Kostrov. In tbe first, stress drop (i.e. loading) was localized to a poine along the crack surface, in which case the crack was predicted to propagatl and, ultimately, arrest. In the second, a uniform stress drop was applied at the crack surface, in which case the crack was found to accelerate towards its limiting speed v_s.

Freund (1972b) and later Fossum and Freund (1975) developed the analogous solutions for arbitrary motion of effectively (i.e. limited by incoming wave arrival times) semi-infinite cracks in modes I and II, respectively. There is found to be a common form of solution, regardless of mode, to the following problem, first enunciated in this form by Eshelby (1969): Let a static, finite crack exist in a body, and suppose the stress distribution along the prospective rupture plane $x_2 = 0$ is $\sigma^0_{2j}(x_1, 0)$. The crack tip is initially at $x_1 = 0$ as in Fig. 3.2.1. Suppose that if rupture extends to a point at x_1 on this plane, the stress there will fall to $\sigma^f_{2j}(x_1, 0)$, and define the stress drop $\Delta\sigma_j = \sigma^0_{2j} - \sigma^f_{2j}$ as earlier. Note that if the crack were to extend by a distance a, the static solution for stress intensity factor would be (e.g. Rice 1968a, eqs. (95), (98))

$$K_j = K_j^0(a) \equiv \sqrt{\frac{2}{\pi}} \int_0^a \frac{\Delta\sigma_j(x_1)}{\sqrt{a-x_1}}\, \mathrm{d}x_1 \tag{3.3.3}$$

if the same stress drop distribution were to act along the prolongation a of a semi-infinite crack. This formula evaluated as $a \to 0^+$ is easily shown to reproduce the stress intensity factors at the original crack tip, contained in the stress distributions $\sigma_{2j}^0(x_1, 0)$. The conclusion of the different analyses cited above by Kostrov, Eshelby, Freund, and Fossum and Freund (see also Kostrov, 1975; Freund, 1976) is that regardless of mode, the dynamic stress intensity factor at the tip of a crack which has grown arbitrarily with time to the amount a, and has instantaneous velocity $v(= \mathrm{d}a/\mathrm{d}t)$, is of the simple multiplicative form

$$K_j = k_j(v) K_j^0(a) \qquad [\text{no sum here on } j] \tag{3.3.4}$$

provided no waves have yet arrived from the other crack tip. The functions $k_j(v)$ can be extracted from the references cited; each begins as unity at $v = 0$ and decreases monotonically to zero at the limiting speed $v = v_r$ or v_s. The expression for mode III is (Eshelby, 1969)

$$k_3(v) = (1 - v/v_s)^{1/2} \tag{3.3.5}$$

Thus, for example, in the case of mode III crack growth the energy release rate is (eq. (3.2.64))

$$\begin{aligned} G &= f_{\mathrm{III}}(v) K_3^2/2\mu = f_{\mathrm{III}}(v)\,[k_3(v) K_3^0(a)]^2/2\mu \\ &= [(1 - v/v_s)/(1 + v/v_s)]^{1/2} [K_3^0(a)]^2/2\mu \end{aligned} \tag{3.3.6}$$

Thus if one regards G as a given constant for rupture propagation or instead, to include spatial heterogeneity and/or rate dependence of fracture resistance, regards G as a function of a and/or v for rupture propagation, eq. (3.3.6) becomes a differential equation describing crack motion. The form makes it evident at once, e.g. that if G is constant for propagation and if $\mathrm{d}K_3^0/\mathrm{d}a$ always is greater than some positive number, then the crack speed accelerates toward v_s. On the other hand if $K_3^0(a)$ diminishes sufficiently with a, crack arrest will occur; this corresponds to a case such as the localized loading discussed above.

The structure of eq. (3.3.6) implies that the effective inertia of a crack tip is zero; a discontinuity in the requisite G along the fracture path causes a discontinuous change in v. This change may possibly be to $v = 0$, i.e. crack arrest, if the discontinuity has the form of a large increase in G, but more generally either discontinuous increases or decreases of v may occur. Husseini *et al.* (1975) have used considerations of crack arrest as discussed above, based on either increases of fracture resistance or decreases of driving force (e.g. localized zone of significant stress drop) to estimate the range of G values cited earlier, Section 3.2.3, from data on nominal stress drops and rupture areas of natural earthquakes.

Similar conclusions on the existence of a limiting speed and lack of effective crack tip inertia follow for rupture dynamics based on the dynamic stress intensity factor, regarded either as constant or as a function of a and v (to include heterogeneity and rate dependence) for rupture propagation. Such may be regarded as a fracture criterion based on critical stress levels ahead of the crack, eq. (3.2.61). However, details of crack acceleration are not the same as for a criterion based on the energy release rate G, as may be seen by comparing the expression for mode III stress intensity factor

$$K_3 = (1-v/v_s)^{1/2}K_3^0(a) \tag{3.3.7}$$

(from eqs. (3.3.4), (3.3.5)) with eq. (3.3.6) for G in the same mode.

Burridge and Halliday (1971) and Achenbach and Abo-Zena (1973) have analysed dynamic crack models of processes occurring in the source of shallow tectonic earthquakes of strike-slip type, analysed as anti-plane strain. Burridge and Halliday (1971) analysed the case of infinite strike-slip fault developing dynamically in a plane perpendicular to the free surface of homogeneous elastic half-space. In their model the crack develops along a plane of material weakness (i.e. pre-existing tectonic fault). Before the initiation of the motion the fault plane is characterized by some distribution of stress σ_{23}^0, variable with depth. The half-space is subjected to hydrostatic pressure (from gravity) and anti-plane shear stresses (tectonic stresses) which increase quasi-statically in time. The initiation of the motion happens locally as a result of a local irregularity of the stress field or coefficient of friction, and sudden slip initiation occurs in the weakened plane. The slipped region develops in both directions (up and down) from the line of slip nucleation. The slipped region reaches the Earth's surface above and stops below at some depth, blocked by the increasing friction. The fracture energy is taken as zero (or negligible) so that from the moment of nucleation both edges of the crack move with the speed of an S-wave. In their work Burridge and Halliday (1971) analyse the motion of both crack edges, assuming that stress drop on a crack surface changes quadratically with depth, so as to turn negative at greater depths. (Negative stress drop means merely that $\sigma_{23}^f > \sigma_{23}^0$, i.e. that the local stress necessary for slip at a point is greater than the stress which acted at that point when rupture initiated elsewhere). They also determine the displacement field on the crack surface as well as deformation field far from the crack, and its dependence on the depth of the nucleation line.

Achenbach and Abo-Zena (1973) analysed two dynamic crack models with geometry and stress fields similar to those modelled by Burridge and Halliday (1971). The first model described the dynamic propagation of an anti-plane shear crack initiated by a shear wave approaching the fault plane. This type of problem might model a shallow earthquake initiated by another earthquake or an underground explosion. The second model described the case solved by Burridge and Halliday (1971), but for a crack with finite length. In both papers the solutions describe the motion of the crack edges and the maximum depth of the slipped region. Also the shear stress distribution on the crack plane after the motion ceased was determined, as well as the displacement along the Earth's surface just above the fault. Comparison of the depth of maximum penetration of the slipped zone for the dynamic case with that obtained in static calculations by Walsh (1968) and Berg (1968) showed that the dynamic analysis gave a slightly greater slip depth.

3.3.2 Numerical dynamic modelling of source processes

The mathematical complexity of crack dynamics limits the usefulness of conventional analytical methods; we review here numerical solutions to such problems and discuss their applications in analysis of earthquake source processes.

It might be advisable in the beginning to notice that there are differences between these two classes of solutions, stemming from requirements of tractability and practicality. The analytical solutions are usually developed with the use of Griffith's theory (i.e. a critical G for propagation, within the assumptions of elastic-brittle crack theory), and under the assumption that in the body analysed there exists one crack in a close-to-critical state, the fracture of the body being described by development of this particular crack. In this approach the presence of other cracks in the material is accepted but not necessary, and usually not taken into account. Crack velocities derived from the elastic-brittle approach are limited to being smaller than the S-wave velocity and, as has been seen, the cracks amenable to analysis are usually semi-infinite or self-similar.

In numerical solutions cracks are usually less large compared to grid size than might be desired, which is the consequence of computer limitations, and, naturally, all quantities are discretized. Some discrepancies between solutions are associated with the fact of discretization, i.e. they depend on the fact that basic equations or quantities at a more advanced level of solution are discretized. Also, some differences stem from the manner of discretization. Moreover, stress concentrations at crack tips are, of course, finite, and the numerical fracture criteria of different kind correspond only approximately, in ways not yet precisely understood, to fracture criteria discussed previously, Section 3.2, in the elastic-brittle context and subsequently, Section 3.4, for more general models. Presumably the process in the earthquake source should *not* generally be modelled by one crack (and its dynamic development) only, but rather, to the extent feasible, one should account for the presence of other cracks (faults) in the medium, as well as for the interaction of cracks between themselves and with the inhomogeneities of material of the Earth and its free surface. Further, non-elasticity of the medium as well as *non*-ideal (i.e. other than elastic-brittle) fracture mechanics should at least sometimes be involved. In principle, numerical solution methods can accommodate such considerations, although practical computer limitations have not yet allowed investigation of all in detail.

A simpler class of numerical solutions is that for which crack motion is specified *a priori* (i.e. no fracture criterion is imposed at the advancing tip) and the (dynamic) stress drop is prescribed along the ruptured surface. For example, Burridge (1969) examined two-dimensional anti-plane and in-plane shear cracks moving at prescribed velocity, and used an integral relationship analogous to eq. (3.2.37) to calculate stress in terms of slip on the crack surface, thereby to formulate an integral equation, discretized and solved numerically, for the slip as a function of position and time. Hanson *et al.* (1974) modelled numerically an analogous problem of unilateral expansion of a two-dimensional shear crack, propagating at constant speed and then stopping.

Also, Madariaga (1976) solved by a three-dimensional finite difference method problems of circular shear cracks in an unbounded elastic medium. In one model a crack with fixed finite dimensions was introduced instantaneously. In another the crack developed from a small nucleation centre with constant speed and then stopped abruptly at some finite radius. Madariaga discussed in detail the wave field far from the moving crack and its dependence on model parameters and the stopping mechanism. No reversal of slip velocity was allowed, in order to simulate the effects of friction, and because of this Madariaga finds that the displacements overshoot those estimated statically, e.g. by eq. (3.2.13) with $\Delta\sigma_1$ identified as the dynamic stress drop. Nevertheless, he finds the spatial distribution over the slip plane to be similar to eq. (3.2.13), the primary difference being that the displacements everywhere are about 15 to 20% larger in the case of a crack growing from a small nucleation centre, and 34% for that introduced instantaneously. Madariaga's work, extended to other applications (Madariaga, 1979; Virieux and Madariaga, 1982) that we discuss subsequently, employs staggered finite-difference grids for particle velocity and stress components.

We consider in the rest of this section numerical dynamic rupture models for which a definite fracture criterion is imposed for crack advance, so that crack motion is not prescribed *a priori*. A formulation for doing this was outlined by Hamano (1974). Basing his numerical procedure on discretization of the integral equation following from the representation of eq. (3.2.39), Hamano prescribed the critical stress level of material along the fault plane. This procedure is particularly simple for numerical applications; it assumes that the crack extends one grid point when the stress at a grid point outside the crack and nearest to the crack tip exceeds the critical value. A similar critical stress criterion, phrased in the context of a two-dimensional finite difference analysis of dynamic tensile cracking, has been proposed by Shmuely and Alterman (1973). The critical stress level within this procedure cannot be interpreted as a true material property. Rather, it is grid-size dependent and must be interpreted in terms of an average of the singular analytical solution over the grid length immediately ahead of the crack tip, as commented by Das (1976) and Das and Aki (1977). In this sense the procedure can be seen as an attempt to simulate numerically the critical stress intensity factor criterion for rupture dynamics discussed in connection with eq. (3.3.7).

However, a detailed study of the critical stress criterion and its numerical applications by Virieux and Madariaga (1982) shows that the procedure duplicates closely the continuum results based on a critical stress intensity factor only over a certain range of parameters. For example, the Das and Aki (1977) dimensionless strength parameter is

$$S = (\sigma_u - \sigma_0)/(\sigma_0 - \sigma_f) \tag{3.3.8}$$

where σ_0 is the remotely applied stress, σ_f the residual friction strength of ruptured portions of the fault, and σ_u is the grid-size dependent critical stress. Virieux and Madariaga find agreement between the numerical critical stress result and that for a continuum with critical stress intensity factor, in the case of Kostrov's (1966) problem of a semi-infinite crack suddenly subjected to the stress drop $\sigma_0 - \sigma_f$, only for the range $3 < S < 7$. They attribute the lower limit to poor numerical resolution of the stress concentration in the then too large grid spacing ahead of the crack; the upper limit apparently reflects the inadequacy of numerical results on a finer grid, at one grid spacing ahead of the crack, to duplicate adequately the near tip elastic singular stress field. Outside these limits the numerical critical stress criterion must be regarded as a separate criterion from those phrased for continuum crack dynamics. However, as pointed out by Vireux and Madariaga (1982), the applicability limits of their numerical rupture criterion are intimately related to the properties of their numerical method (finite difference method) and it may happen that other numerical methods proposed in the literature have different limits of applicability.

Andrews (1976) combined a finite difference technique with the slip-weakening fracture criterion of Ida (1972) and Palmer and Rice (1973) to solve for the rupture propagation of a finite, two-dimensional shear crack in an infinite medium. The criterion is discussed in Section 3.4.1 and is consistent with a Griffith-like criterion of critical fracture energy G when the slip-weakening zone is small compared to all other scale lengths in the problem. For the case of in-plane shear crack Andrews showed that the terminal rupture velocity could be smaller than the Rayleigh velocity or higher than the shear wave velocity, depending on the strength of the material on the fault plane. The same was confirmed in subsequent three-dimensional finite difference implementations of the criterion by Day (1982b). Burridge *et al.* (1979) observe that for a mode II crack propagating at speeds near v_r consistently with a slip-weakening zone at its tip, large shear stresses exists on the prospective rupture plane ahead of the slip-weakening zone and, as found numerically by Andrews, these stresses may be of sufficient magnitude to exceed the peak stress necessary to initiate slip. In that case a disconnected zone of slip develops ahead of the main rupture, coalescing with it in an unsteady manner and allowing, ultimately, the steady spread of rupture at speeds exceeding approximately $1.5v_s$.

Similar features appear in numerical simulations of in-plane shear rupture based on the critical stress criterion. However, as pointed out by Virieux and Madariaga (1982), such features, including transonic rupture velocities, are intrinsic to the numerical method only, and would not appear in analytical solutions based on a critical K criterion, which the numerical stress criterion is intended to simulate. The numerical stress concentration at the rupture front represents actually a numerical coalescence of the crack stress concentration and that of the strong S-wave peak ahead of the crack tip. As noted earlier, analytical solutions are not necessarily in simple correspondence with numerical solutions, and the differences can become particularly notable when prediction of rupture propagation is included. For example, in the case under discussion, it happens that in the analytical approach the rupture front singular stress concentration is separated from the S-wave peak and only the rupture front stress concentration is used in the calculation of the maximum rupture velocity. In the numerical method, at high rupture velocities of in-plane cracks, the S-wave stress peak coalesces with the rupture front stress concentration, giving rise to transonic rupture velocities.

An extensive numerical study of the development of shear cracks as applied to the analysis of earthquake source mechanisms has been presented by Das (1976). The author considers consecutively three important problems, namely the process of unilateral spontaneous development of a finite shear crack in an infinite elastic body, the influence of barriers (obstacles) laying in the plane of the developing crack on the shape of near- and far-displacement fields, and the stopping mechanisms for finite shear cracks moving in an infinite elastic body. As a fracture criterion the postulate of a critical stress, as introduced by Hamano (1974) and discussed above, was used. Work by Das (1976) has been extended in studies by Das and Aki (1977a, b) and Aki (1979). For the first time in the modelling of earthquake source processes the possibility of the propagation of not only one, but a few cracks, developing consecutively (model with barriers) was taken into account. Also, a detailed analysis of the influence of stopping mechanisms on the deformation field near and far from the developing crack was presented. The above results are particularly interesting for the mechanics of earthquake source processes, thus we will discuss them here in some detail.

Analysing numerically bilateral dynamic development of an in-plane shear crack starting from the Griffith critical length and controlled by the critical stress fracture criterion, Das (1976) and Das and Aki (1977) found that, depending on the strength of the material (given by the critical stress jump) and the instantaneous length of the crack, the propagation velocity of the crack-tip could be sub-Rayleigh or super-shear, and, for low strength materials, could even reach the P-wave velocity. This phenomenon is caused by the fact discussed above that the value of critical stress-jump could be overstepped by the dynamic stresses caused by P- and S-waves travelling in front of the developing crack-tip which could cause the increase of crack velocity to values higher than the S-wave velocity, as obtained also by Andrews (1976) with the slip-weakening model. It is interesting to note that a tensile (opening) crack developing under identical conditions could not reach velocities higher than Rayleigh wave velocity in numerical simulations, because the stress field before the crack tip tends to close the crack, which arises from the Green's function for that problem (see Hamano, 1974).

Das (1976) and Das and Aki (1977) also show that in the case of smooth crack development (that is, with no barriers of higher material strength in the crack plane) the crack starts with some small velocity but then accelerates rapidly to its terminal velocity, determined by strength distribution in the crack plane, and thus the average rupture velocity over an entire length of fault cannot be much smaller than the terminal velocity. Only the presence of barriers along the path of the developing crack could decrease the average rupture velocity significantly.

Using the model of dynamic propagation of an in-plane shear crack with finite dimensions and the information that for most earthquakes studied so far the rupture velocity is less than the shear wave velocity (see Tsai and Patton (1972), Eaton (1967), Kanamori (1970a, 1970b, 1971, 1972), Takeuchi and Kikuchi (1973), Wu and Kanamori (1972), Niazy (1975), Aki (1968), and others), Das (1976) estimates the fracture energy for the case of strong shallow earthquakes with long ruptures and obtaind the value of $10^7\ \mathrm{J \cdot m^{-2}}$. A similar value has been estimated by Ida (1973), from the observed maximum seismic motion due to an earthquake. Independently, Takeuchi and Kikuchi (1973) also proposed a similar value, based on a rough estimate of the time needed for the rupture velocity to approach the terminal velocity.

Das (1976) and Das and Aki (1977) introduce the concept of a shear fault developing dynamically through obstacles (barriers) in the plane of the growing rupture, consisting of material of some higher strength. After the passage of the fault the barriers could be left intact, or they could break either during the fault motion, or some time after it (very short time aftershocks), depending on the ratio of the strength of barrier to the tectonic stress acting in the region. The model offers an explanation for a variety of observations of processes in earthquake sources. These include, among others, fault segmentation observed at the time of some earthquakes and in regions of rockbursts in mines, some characteristics of seismograms which could not be explained as effects of wave propagation in the medium only, and also discrepancies of observations of seismic wave spectra from the spectrum based on similarity of earthquakes of different magnitudes. Also, the model explains why in some particular cases the simple Volterra dislocation constitutes a better model of source process than a crack model without barriers. The model predicts that earthquakes with low average stress drop could generate more waves with higher frequencies than earthquakes with high stress drops. Also, an important conclusion stemming from the concept of a fault with barriers is the possibility of prediction of aftershocks based on analysis of the shape of the seismic pulse generated by the main shock.

In their model of a fault with obstacles (barriers) Das (1976) and Das and Aki (1977b) consider the problem of unilateral propagation of an in-plane shear crack in an unbounded homogeneous elastic medium, using the criterion of critical stress jump introduced by Hamano (1974). The medium is initially under a uniform shear stress σ_0; the fault slip starts as the shear stress across the fault plane exceeds some value σ_u, and then

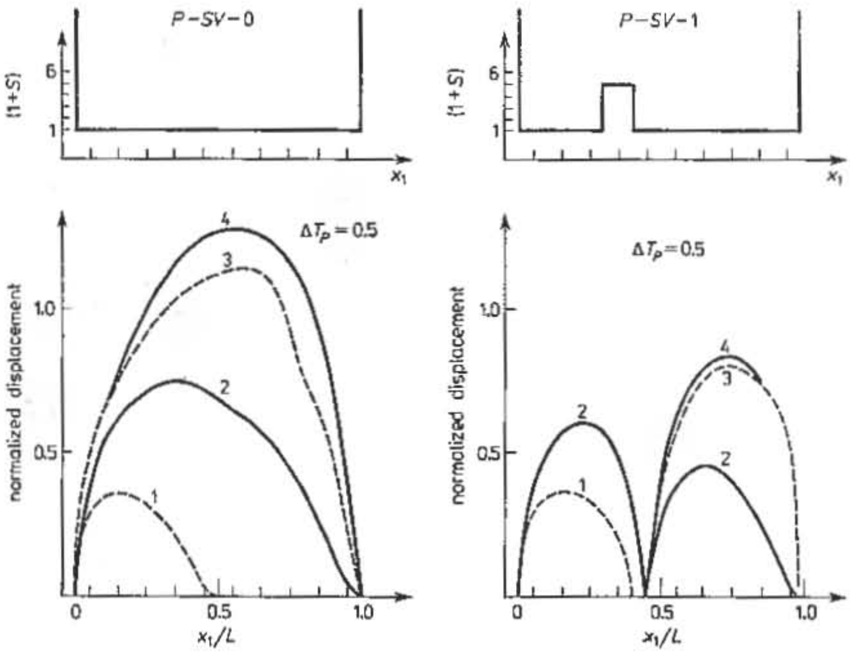

Fig. 3.3.2. The value of $(1+S)$, a measure of material strength relative to tectonic stress as defined in eq. (3.3.9), is shown as a function of distance x_1 along the path of rupture propagation at the top of the figure. This is case *P-SV*-0, in which no barriers exist on the fault plane. At the bottom snapshots of the parallel component displacement on the crack surface $u_1(x_1, 0, t)$ are shown as a function of x_1; u_1 is normalized by factor $L(\sigma_0-\sigma_f)/3\mu$, and the number beside each curve indicates time t measured in the unit of $0.5\,L/v_p$, where L is the length of the fault, v_p is the compressional wave velocity, μ is the rigidity, σ_0 is the initial tectonic stress, and σ_f is the dynamic friction of the fault plane (after Das and Aki, 1977b; copyrighted by the American Geophysical Union). Fig. 3.3.3. Case *P-SV*-1, in which one barrier exists on the fault plane. See Fig. 3.3.2 legend for details. The crack tip skips the barrier without breaking it (after Das and Aki, 1977b; copyrighted by the American Geophysical Union).

its value drops to the dynamic frictional stress σ_f. The slip motion is frozen once the slip velocity begins to change sign.

The authors introduce the non-dimensional parameter S of eq. (3.3.8), being a measure of material strength relative to tectonic stress, and parameterize rupture resistance in terms of

$$1+S = \frac{\sigma_u-\sigma_f}{\sigma_0-\sigma_f} \tag{3.3.9}$$

Barriers along the fault plane are characterized by high values of parameter $(1+S)$. In their simulations Das (1976) and Das and Aki (1977b) considered only cases where $S = 0$ everywhere over the region to be ruptured except on barriers. The crack starts from a point and is stopped after 10 grid points. They consider the following four cases of barrier distribution:

P-SV-0: No barriers, as shown in Fig. 3.3.2.

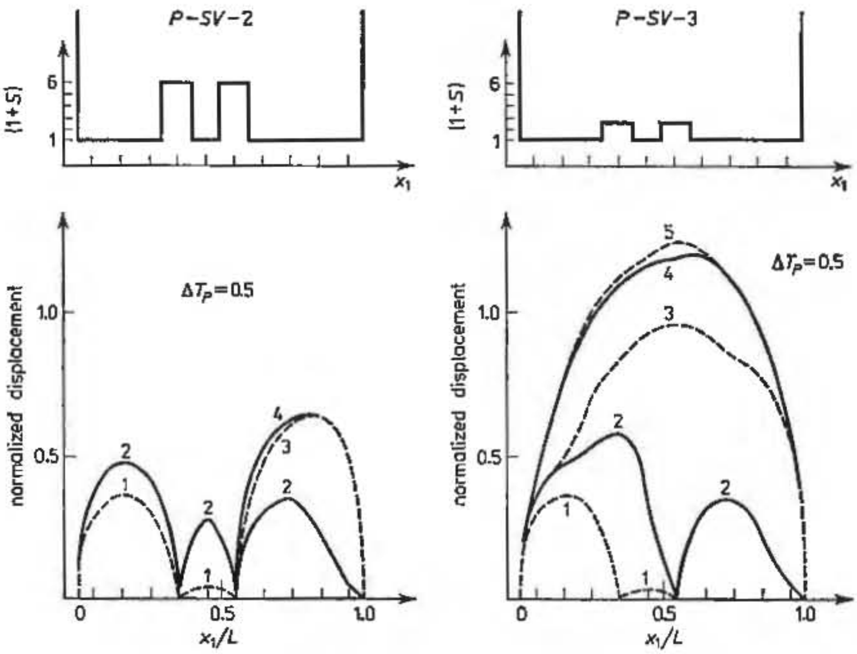

Fig. 3.3.4. Case *P-SV*-2, in which two barriers exist on the fault plane. See Fig. 3.3.2 legend for details. The crack tip skips the barriers without breaking them (after Das and Aki, 1977b; copyrighted by the American Geophysical Union).

Fig. 3.3.5. Case *P-SV*-3, in which two barriers with a smaller value of $(1+S)$ than was used in *P-SV*-1 or *P-SV*-2 exist. See Fig. 3.3.2 legend for details. In this case the barriers are eventually broken (after Das and Aki, 1977b; copyrighted by the American Geophysical Union).

P-SV-1: One barrier with $1+S = 5$ exists at a grid point on the fault plane (Fig. 3.3.3). The crack leaves the barrier unbroken.

P-SV-2: Two barriers with $1+S = 6$ exists at two separated grid points. The barriers are unbroken (Fig. 3.3.4).

P-SV-3: Two barriers with $1+S = 2.5$ exist at the same grid points as in the previous case (Fig. 3.3.5). The barriers are not broken at the time of passage of the rupture front but are broken before completion of the rupture process.

The crack develops along the x_1-axes; Figs. 3.3.2, 3.3.3, 3.3.4 and 3.3.5 represent the displacement $u_1(x_1, 0, t)$ on the crack surface as a function of x_1 for a fixed time t for different cases of barrier distribution. The number by each curve indicates the time in the unit of $0.5L/v_p$, where L is the fault length and v_p is the compressional wave velocity. Displacement u_1 is normalized by the factor $L(\sigma_0-\sigma_f)/3\mu$. In all cases the crack tip propagates with a velocity v_p because $S = 0$ at all grid points except barriers. Let us note that in the case when barriers are left unbroken (Figs. 3.3.3 and 3.3.4), the displacement field is somewhat similar to that of a Volterra dislocation model (Haskell model). In the case when barriers are broken (Fig. 3.3.5) the history of the deformation process is more complex and the final slip is reached after a slightly longer time.

The influence of presence as well as strength of barriers on far-field wave forms is illustrated in Figs. 3.3.6–3.3.9 for comparison, the dashed lines show the curves for case *P-SV*-0 (without barriers).

The excitation of high-frequency waves is relatively greater in cases when the barriers remain unbroken, in comparison with cases when barriers break. However, the amplitude spectrum does not clearly reveal the complexity of damage processes occurring in the rupture plane in presence of barriers and it does not show clearly any difference between particular cases. These differences however could be detected by studies of shape of the seismic pulse; in the case without barriers (Fig. 3.3.6) the pulse is smooth except for the sudden arrival of stopping phase generated by the moving crack edge, and in case *P-SV*-3 (Fig. 3.3.9) it is highly disturbed by many small ripples, observed in all directions. Note that these differences are not seen clearly when comparing the amplitude spectrum only (Das and Aki, 1977).

The analysis performed by Das (1976) and Das and Aki (1977) suggests that if the barriers are unbroken, the directivity of the seismic radiation is somewhat stronger than that for the rupture without barriers. Also they argue that the presence of barriers might cause the slowdown of the rupture process as well as a slight decrease of corner frequency averaged

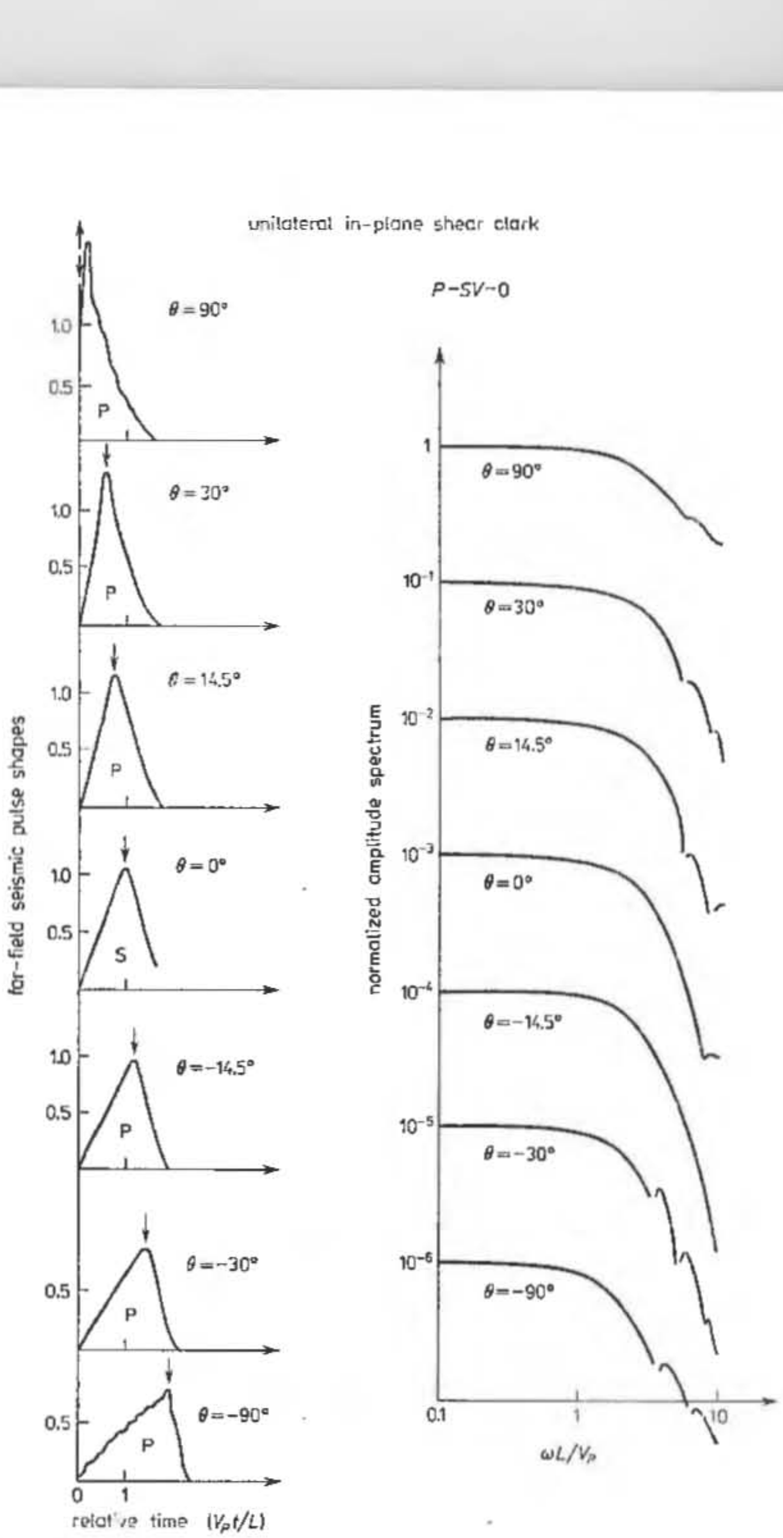

Fig. 3.3.6. Left: The far-field wave form $f(\theta, t)$ is shown for P-waves for various values of θ for case P-SV-0. The arrows indicate the arrival of stopping phase from the moving crack tip. Right: The absolute value of the Fourier transform of $f(\theta, t)$ is shown in a logarithmic scale normalized to the value at zero frequency (after Das and Aki, 1977b; copyrighted by the American Geophysical Union).

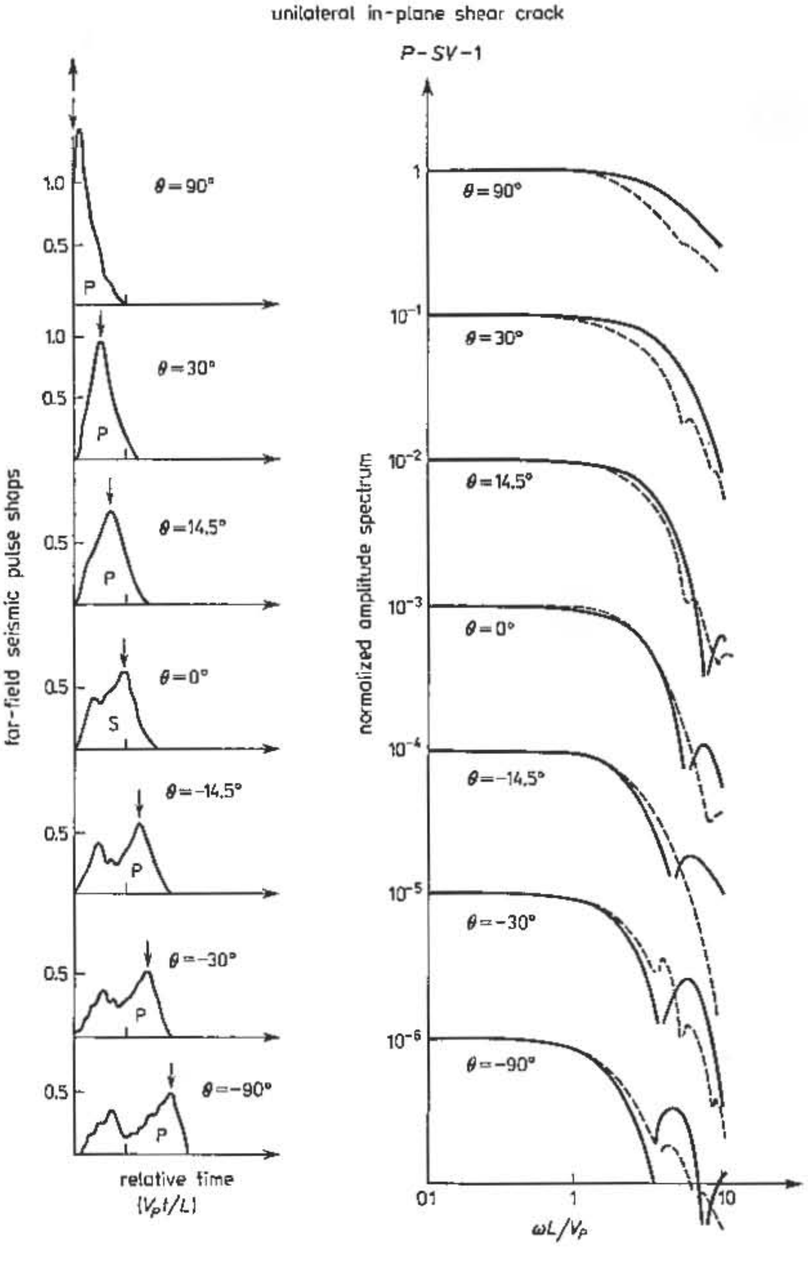

Fig. 3.3.7. Case *P-SV*-1. See Fig. 3.3.6 legend for explanation and symbols. For comparison, the dashed lines on the figure of the spectrum show the curves for case *P-SV*-0 (after Das and Aki, 1977b; copyrighted by the American Geophysical Union).

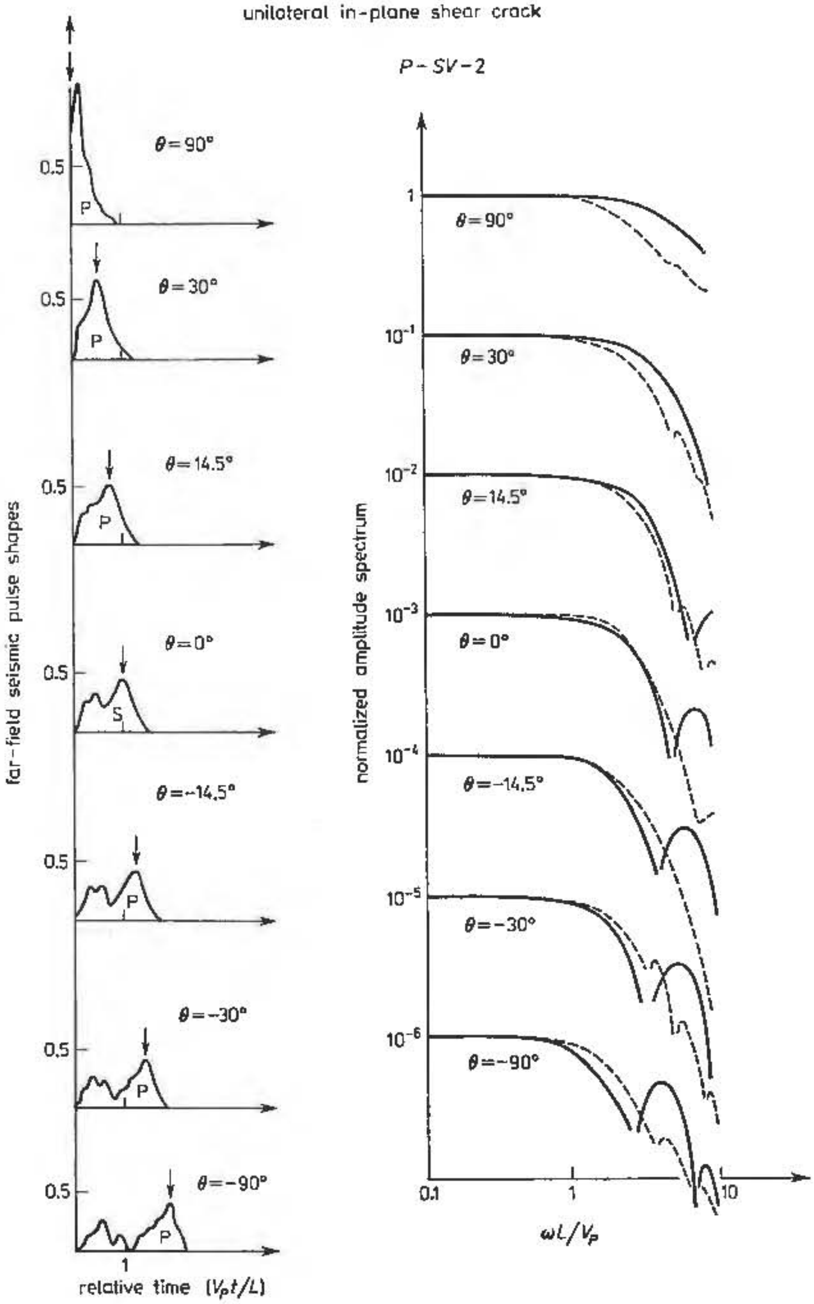

Fig. 3.3.8. Case *P-SV*-2. See Fig. 3.3.6 legend for explanation of symbols. For comparison, the dashed lines show the curves for case *P-SV*-0 (after Das and Aki, 1977b; copyrighted by the American Geophysical Union).

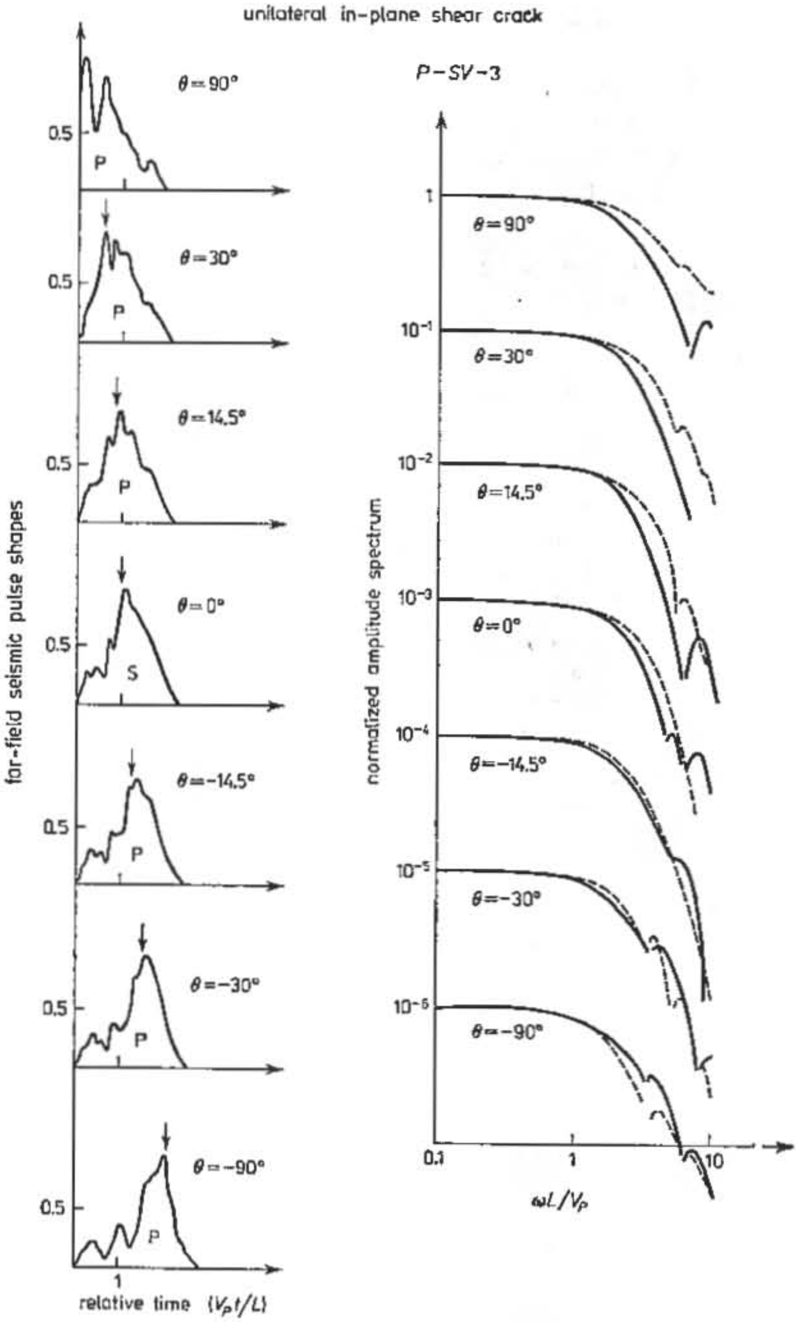

Fig. 3.3.9. Case *P-SV*-3. See Fig. 3.3.6 legend for explanation of symbols. For comparison, the dashed lines show the curves for case *P-SV*-0. The far-field wave forms show ripples in all directions (after Das and Aki, 1977b; copyrighted by the American Geophysical Union).

over all directions, which happens in cases when barriers remain unbroken with the passage of rupture front but eventually break, too. They thus associated the corner frequency more with the amount of time needed for the completion of rupture process than with the total length of the broken region.

The numerical modelling of the earthquake source process as performed by Das (1976) and Das and Aki (1977) offers the possibility of leaving one or more intact regions along the path of the developing rupture (fault segmentation). Although when examining the surface traces of faults produced by shallow strong earthquakes, it is difficult to estimate the complex structure of subsurface layers, in some cases fault segmentation might be associated straightforwardly with surface kinks or segments of the main fault itself (see, e.g. Imperial Valley earthquake of 1940, Richter (1958), Trifunac and Brune (1970); Dasht-e Bayaz earthquake of 1968, Tchalenko and Berberian (1975)). Also examination of the first unearthed rockburst fault from a deep gold mine in South Africa (Spottiswoode and McGarr, 1975) revealed clear segmentation of the fracture areas. Thus the barrier model offers a simple mechanical basis for so-called "multiple ruptures" (Stoneley, 1937; Usami, 1956; Wyss and Brune, 1967; Trifunac and Brune, 1970; Kanamori and Stewart, 1976). Of course, the physical basis for segmentation may not be related to such strong initial non-uniformity of material strength properties. Possibly, dynamic ruptures in a simple planar form are configurationally unstable, e.g. Rice (1980) and Section 3.4.1.

The barrier model also offers a basis to interpret small impulses observed in some cases in the early parts of seismograms (Kasahara, 1956; Rulyov, 1975), which could not be attributed to wave transmission properties of the medium alone. These impulses are probably associated with the rupture front passing through the barrier, which was suggested by Rulyov (1975) when interpreting seismograms of one of earthquakes from Garm (Tadzhikistan) region.

One consequence of the idea of a fault plane with barriers is the creation of a physical basis for description of the faulting process in such a way that the average slip along a long fault is of similar magnitude everywhere. Considering a long fault with strong (unbreakable) barriers distributed in a more or less uniform way along the fault, we obtain a locally heterogeneous slip distribution which in average is similar to the classical dislocation model. This would resolve the situation that the simple dislocation model of a source process, introduced by Ben-Menahem (1961) and Haskell (1964) and subsequently criticized for its insufficient physical basis (Sato and Hirasawa, 1973; Molnar *et al.*, 1973), in some cases explained much better the existing observational data than the crack model without barriers (see e.g. Parkfield earthquake of 1966, Aki, 1968; Archuleta and Brune, 1975). Recently Bouchon (1977) observed that in the case of the 1971 San Fernando earthquake, a crack model without barriers is not able to explain observed far-field wave recordings, whereas a model with unbroken barriers (of type *P-SV*-1 or *P-SV*-2) gives a wave field similar to that generated by a Volterra dislocation model and compatible with recordings of this earthquake.

The barrier model of the source process allows also prediction of aftershock occurrence, with the use of analysis of the shape of the seismic pulse generated by the main shock. Unbroken barriers are naturally regions of stress concentration and possible sources of subsequent shocks (aftershocks). If the barriers were completely broken during the main rupture process, then it is possible that aftershocks (or at least strong ones) would not occur at all within the main rupture zone. The lack of aftershocks of medium-deep and deep earthquakes might thus be caused by homogeneity of strength distribution in the region of fracture (see Das and Aki, 1977).

One of the important problems of the physics of an earthquake source is the understanding of the stopping process for an earthquake rupture. Analysing the development of semi-infinite longitudinal shear cracks in an infinite elastic medium Husseini *et al.* (1975) proposed two different stopping mechanisms, as remarked in Section 3.3.1. The first one, called the "fracture energy barrier mechanism", operates when the developing crack encounters on its way a region (barrier) with higher fracture energy (material with higher strength). The second mechanism, called the "seismic gap mechanism", operates when the initial higher tectonic stress field is limited to some finite region, so that when the rupture travels outside that region into area with comparatively lower initial stress levels, it slows down and stops completely.

Both mechanisms of rupture arrest were investigated and compared in work by Das (1976) for a case of a finite shear crack. The author analysed the one- and two-directional development of shear cracks of both kinds (transverse and longitudinal shear), showing how both stopping mechanisms operate in the case of finite cracks. For the "seismic gap" mechanism the crack, encountering the region with lower stresses, moves for some time into it and then stops. The comparison of results for finite cracks with those for semi-infinite ones (Husseini *et al.*, 1975) suggests that the relation between fracture energy, stress drop on a crack and its dimensions proposed by Husseini *et al.* (1975) corresponds only approximately to the finite crack results (see Das, 1976). Such may, however, be due to the difference in fracture dynamics for critical G versus critical K criteria, compare eqs. (3.3.6) and (3.3.7), or to discrepancies between the latter criterion and the numerical critical stress criterion. The stopping mechanism of a fracture "energy barrier" type operates also for finite cracks (Das, 1976) and for a given initial crack length and given position of the barrier, the difference between strength of material of the barrier and that of the crack plane determines if the crack would stop or not.

It is interesting to compare both mechanisms for the same initial crack length, as was done by Das (1976). In the "seismic gap" stopping model the crack edge slows down and then stops, the stopping process being irregular and generating high frequency waves. In the case when the crack encounters a barrier with higher strength, the stopping part of the process is quite sudden and only the very last phase generates high frequency waves. Also the final displacement at crack's edge is larger than in the "seismic gap" stopping model. On the other hand, the stopping mechanism doesn't influence significantly the value of displacement in the middle regions of the ruptured zone (Das, 1976).

A gradual, slower stopping process gives a lower corner frequency value than for a smooth rupture with sudden crack arrest. Normalized far field spectra for both stopping mechanisms are shown in Fig. 3.3.10, where

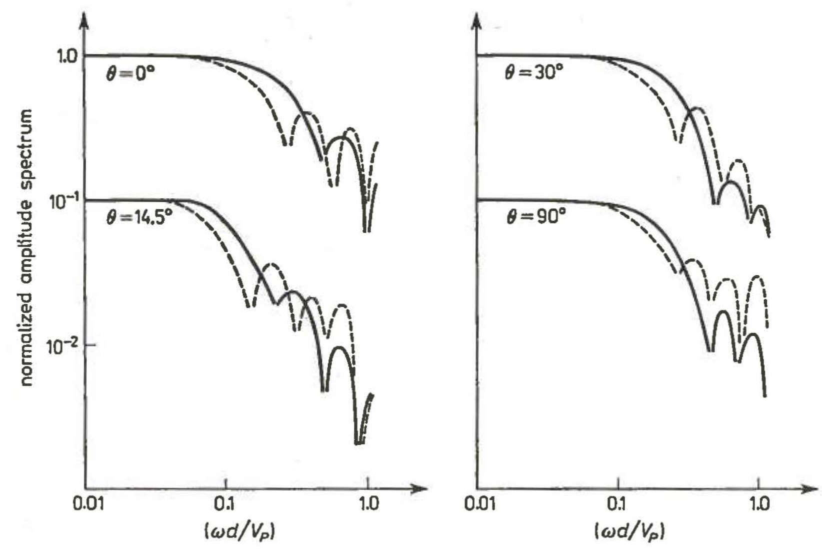

Fig. 3.3.10. Far-field spectra for the case when the tip stops abruptly (solid line) and when it stops gradually (dotted line) for different values θ (after Das, 1976).

the solid line denotes the case when the crack tip stops abruptly (energy barrier mechanism) and the dotted line results from the case when it stops gradually (seismic gap mechanism). Because the final value of displacement at the crack's edge is different for different mechanisms, the factors normalizing the amplitude spectra are different too. The high frequency asymptote of the amplitude spectrum decays as ω^{-2} in case of sudden arrest and as ω^{-1} in case of gradual stopping (Das, 1976). Madariaga (1976) has shown on theoretical grounds that a spectrum decay as ω^{-2} must accompany the sudden stopping of a crack.

Let us return now to the maximum stress criterion as used by Das and Aki (1977), and, also, by Shmuely and Peretz (1976), Mikumo and Miyatake (1979), Day (1979), Das (1981) and Miyatake (1980). It has been pointed out by Das and Aki (1977) that the criterion is equivalent to a critical stress intensity criterion through a relation of the form

$$\sigma_u = \sigma_f + 2K_{cr}(2\pi d)^{-1/2} \tag{3.3.10}$$

where σ_u is the grid-size dependent critical stress, σ_f is the residual friction strength, d is the grid-size, and K_{cr} is the critical stress intensity factor. Thus implicit in the definition of the maximum critical stress there is a scale length that Das and Aki (1977) took as the grid spacing d. Virieux and Madariaga (1982) emphasized in the analysis of spontaneous propagation of finite cracks, that the scaling relation for the maximum stress, in terms of the non-dimensional critical stress intensity factor $K_t = K_{cr}/\sigma_e L^{1/2}$, can be rearranged as

$$\sigma_u = \sigma_f + 2\sigma_e K_t(L/2\pi d)^{1/2} \tag{3.3.11}$$

where L is the length of crack and σ_e is effective stress ($\sigma_e = \sigma_0 - \sigma_f$). The form of eq. (3.3.11) makes it clear that for a finite crack the maximum stress criterion depends on the number of grid points inside the crack (L/d). Thus, as pointed out by Virieux and Madariaga (1982), for a given maximum stress intensity, the finer the numerical mesh, the higher the maximum stress that has to be adopted.

Because of their complexity, three-dimensional crack models of the earthquake source process were attempted only recently and, obviously, only numerically. A major difficulty (but not the only one) with three-dimensional numerical solutions is the need of large computer capacity; some authors avoided this problem by studying models possessing a certain symmetry, as Madariaga (1976) did in the case of circular cracks or by making approximations (Mikumo and Miyatake, 1979) in order to reduce the three-dimensional problem to a two-dimensional one. The truly three-dimensional solutions have been determined by Archuleta and Frazier (1978), Archuleta and Day (1980), Das (1980) and Day (1982a), who studied shear cracks developing with arbitrarily assigned rupture velocities, with the use of finite difference techniques, or, in case of Das (1980), applying boundary integral equations. Spontaneous three-dimensional solutions have been proposed by Day (1979), Miyatake (1980), Das (1981), Virieux and Madariaga (1982) and Day (1982b). This last class of solutions is most valuable for realistic modelling of the earthquake source process since dynamic development of the crack is not prescribed in advance, but rather controlled by the rupture criterion.

Numerical solutions for prescribed rupture velocities on dynamic faults, although not being very realistic in modelling real earthquake source processes, have satisfactorily quantified some important three-dimensional geometrical effects such as the influence of fault width on the slip function. For example, Day (1982a) obtained closed-form approximations for the dependence of final slip, slip rise time, and slip velocity intensity (i.e. the strength of the crack-edge velocity singularity) on fault width and length. By means of such relationships, the fixed rupture velocity dynamic models help establish physical interpretations for the purely kinematic parameters associated with the dislocation earthquake models used more routinely in seismology.

Numerical three-dimensional solutions of spontaneous rupture propagation, though still few in number, are presumably the best approximations to real earthquake source processes. The most complex model has been presented recently by Day (1982b), who studied the effects of non-uniform prestress on spontaneous development of shear cracks with the use of the slip-weakening failure criterion (as in Ida, 1972; Palmer and Rice, 1973 or Andrews, 1976) and a finite difference method. As for two-dimensional numerical simulations of spontaneous propagation of shear cracks, he obtained super-shear rupture velocities for three-dimensional cracks in directions for which mode II (in-plane) crack motion dominates, and sub-shear velocities for directions of predominantly mode III (anti-plane) crack motion. Introduction of even relatively simple stress heterogeneities on the plane of the developing crack made the rupture histories fairly complex (as did barriers in the two-dimensional analysis of Das and Aki, 1977) and in all cases studied, it was sufficient to reduce the *average* rupture velocity to less than the S velocity, although locally super-shear rupture velocities were occurring in regions of high prestress. As proposed by Day (1982), results of this numerical simulation of the earthquake source process could be used to synthesize the radiated seismic wave field with the use of slip histories obtained; this would shed some light on understanding rupture histories of real earthquakes.

3.4 INSTABILITY IN RELATION TO THE CONSTITUTIVE DESCRIPTION OF FAULT SLIP

In this section we examine an approach to fracture analysis which recognizes that the tractions σ_{2j} on a rupturing fault surface should not be regarded as specifiable, *a priori*, but rather should be regarded as being given by some suitable constitutive relation between them and the fault slip Δu_j. An attribute of such a constitutive relation, if it is to describe processes normally understood as shear fracture, is that the resistive stress σ_{21} (say, for the mode II crack, Fig. 3.2.1) must decay from some relatively high peak strength, necessary to get slip started, down to some reduced stress, of the sort we have denoted by σ_{21}^f, on well-slipped segments of fault. This strength decay is, after all, what is meant by fracture. In the simplest group of models, namely, those called "slip-weakening" models, the stress σ_{21} at a given location along a fault is assumed to be some decreasing function of the amount of slip, Δu_1, at that place, at least for slip at constant effective normal stress. More generally, however, it is evident that rate and/or time dependence must be a feature of a suitably complete constitutive description. For example, earthquakes do recur on the same portions of faults, and this suggests that some process of regaining strength can take place on a segment of fault surface in stationary, or nearly stationary, contact. The same regaining of strength can be inferred on the laboratory scale, where repeated stick-slip instabilities can be induced on, say, a saw-cut surface in a continually shortened triaxial specimen within a sufficiently soft loading apparatus. Thus, after consideration of slip-weakening models in the next sections we examine more comprehensive "slip-rate and surface-state" dependent constitutive models and discuss their implications for instability.

The viewpoint adopted in this section is distinct from that of elastic-brittle crack mechanics. In the elastic-brittle approach, the resistive stress is assumed to drop instantaneously, at all points behind the advancing crack tip, to the constant or perhaps slowly varying value σ_{21}^f (again for the mode II crack) and to be unbounded at the tip, the admissible magnitude of the tip singularity being specified by assumption of a critical value G or K, which may include some rheological features through a presumed dependence on speed v. Nevertheless, it is to be expected that the more detailed approach outlined in this section is consistent with elastic-brittle analysis procedures in the limiting case when severe drops in resistive strength σ_{21} occur over a zone near the advancing crack tip that is some small fraction of overall crack size. This expectation is confirmed, at least in the context of slip-weakening models, and in the process one obtains an interpretation of the critical G quantity of the elastic-brittle approach.

The approach of this section continues to represent the fault as a plane of discontinuity in Δu_j (precisely, in its slip components Δu_1, Δu_3), and the constitutive relations to be discussed relate σ_{21}, σ_{23} along the fault to these slips. In principle, the material outside the fault could have any particular constitutive character. Most studies have been limited to the assumption of elastic behaviour and the same assumption is made here. As commented in the Introduction, however, the study of a wider range of rheological models may have significance for earthquake phenomena.

Figure 3.4.1 shows a slipping region along a fault and, in enlarged view, there is shown a small area segment of the fault along which stress and other constitutive parameters can be considered as being sensibly uniform at the continuum scale adopted. The fault surface is regarded as

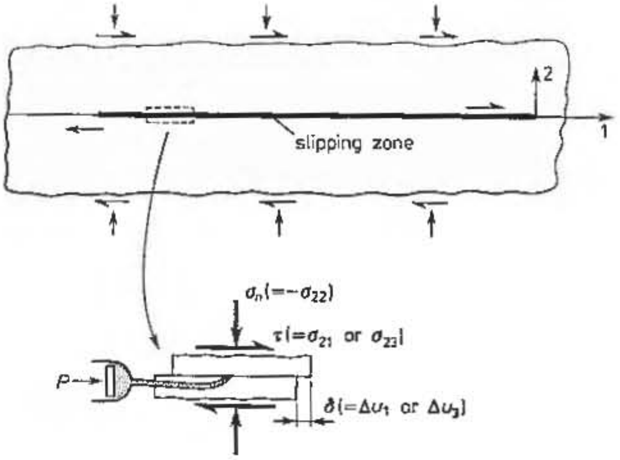

Fig. 3.4.1. Slipping region along fault surface and enlarged view showing parameters entering constitutive description.

a plane of discontinuity of amount δ in sliding displacement, where δ is to be understood as representing, in different circumstances, either Δu_1 or Δu_3 or some linear combination of the two. The shear stress transmitted across a given segment of fault is denoted by τ, which may represent either σ_{21} or σ_{23} or some linear combination. Other parameters of interest to a constitutive description are normal stress $\sigma_n(= -\sigma_{22})$ and, in cases for which it is sensibly defined, the pore-fluid pressure p along the fault surface. Temperature is, of course, also relevant but is considered only implicitly here.

3.4.1 Slip-weakening fault instability models

Figure 3.4.2*a* illustrates a rate independent constitutive relation between τ and δ. This incorporates slip-weakening, and response is of the rigid-plastic type in that unloading and reloading occur along a vertical line segment as shown. As indicated, τ^p denotes the peak slip resistance and τ^f the residual frictional resistance which results after suitably large slip, say, of amount δ_*. Figure 3.4.2*b* emphasizes that τ^p, τ^f and the level of τ at any slip δ must be regarded as being dependent on the effective normal stress $\bar{\sigma}_n(=\sigma_n-p)$. Presumably, the difference between τ^p and τ^f should be assumed to decrease with increasing temperature, and to first increase but later decrease with increasing $\bar{\sigma}_n$ (transition from cataclastic to ductile flow). Thus recognizing that σ_n and temperature both increase with depth

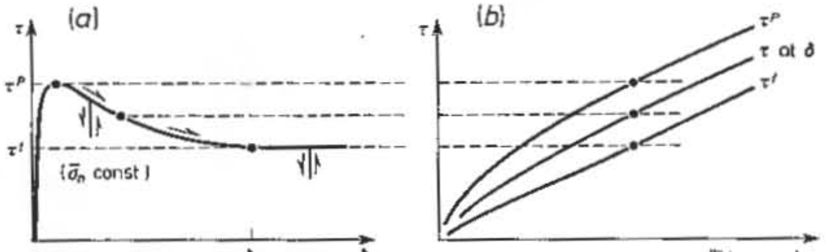

Fig. 3.4.2. Slip-weakening model. (*a*) $\tau=\hat{\tau}(\delta)$ for continued slip at $\bar{\sigma}_n$ constant; (*b*) the $\tau\delta$ curve depends on $\bar{\sigma}_n$.

(anomalous local pore pressure zones may cause $\bar{\sigma}_n$ not to do so monotonically) and assuming that the rate independent constitutive framework adopted is an appropriate approximation for all depths of interest, the difference $\tau^p-\tau^f$ should first increase with depth and then diminish with greater depth. The zone of high brittleness (i.e. substantial $\tau^p-\tau^f$) thereby defined models the seismogenic layer of the Earth's crust.

Simple descriptions of instability according to the slip-weakening constitutive model can be given in the two limiting cases of essentially uniform slip and of highly non-uniform slip, the latter being so much so that results for the slip-weakening model become coincident with those of elastic-brittle crack mechanics. We discuss both limiting cases here in the simple circumstances of failure at fixed effective normal stress $\bar{\sigma}_n$.

The presumption of essentially uniform slip everywhere on a given fault segment is evidently inconsistent with the fact that natural fault segments have ends at which slip must diminish to zero. Further, it is not the type of rupture mode exhibited for large systems, which tend towards non-uniformity of slip approaching crack-like response. However, such essentially uniform slip could, for example, be exhibited if a small enough segment of fault were cut free, as in the enlargement in Fig. 3.4.1, and subjected to laboratory test as a specimen with a throughgoing fault. Also, the description of instability that results based on this assumption of uniform slip finds application in less restricted analyses of failure in slip-weakening or other deformation-weakening systems (Jaeger and Cook, 1979; Rudnicki, 1977; Rice, 1979; Stuart 1979a, b; Stuart and Mavko, 1979; Li and Rice, 1983).

From a dynamical viewpoint, an elastic system that either exhibits or is idealized as exhibiting uniform slip motion can be regarded as a single degree of freedom elastic system, and can be represented schematically by a spring-slider system as in Fig. 3.4.3*a*. There δ denotes the slip, and the force T per unit base area of the slider, exerted on it by imposed displacement δ_0 of its surroundings, is represented by the linear spring force

$$T = k(\delta_0 - \delta) \tag{3.4.1}$$

where k is the elastic stiffness. For quasi-static response of the spring-slider system, $\tau = T$. In some circumstances it is more appropriate to regard τ_0 as the prescribed quantity where τ_0, replacing $k\delta_0$, is the stress exerted on the slider in the absence of slip. Then one writes, for quasi-static conditions

$$T = \tau = \tau_0 - k\delta \tag{3.4.2}$$

which may be regarded as the one-dimensional form of the general relation between stress and slip in eq. (3.2.25).

Figures 3.4.3*b* and 3.4.3*c* illustrate the solution under increasing imposed displacement δ_0. The straight lines are plots of eq. (3.4.1), with $T = \tau$, for various values of δ_0. Their intersections with the τ versus δ relation define the state of the system. Thus, as δ_0 is increased, slip is stable in a stiff system, Fig. 3.4.3*b*, but becomes unstable in a softer system, Fig. 3.4.3*c*, when the τ versus δ relation falls at a slope greater than the spring stiffness.

Figure 3.4.3*d* shows (as points B, C, D, E) possible final states of the system after an instability. Their range is determined by the conditions that

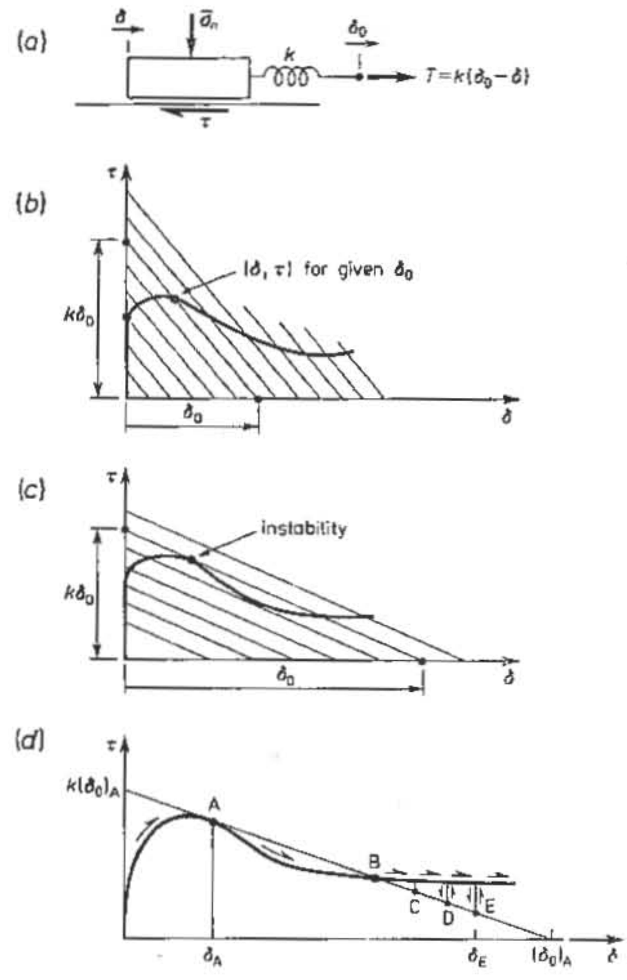

Fig. 3.4.3. (*a*) Spring-slider representation of single degree of freedom elastic system, appropriate for uniform slip. (*b*) and (*c*) Successive stress and displacement states encountered as load-point displacement δ_0 is increased; stable for high stiffness in (*b*), unstable for low stiffness in (*c*). (*d*) Points B, C, D, E show possible final states after dynamic instability, depending on amount of energy radiated away; point E is such that the area under line AE equals that under the τ versus δ relation between δ_A and δ_E.

(i) the final state be a possible equilibrium state, and

(ii) the energy lost from the system (in representation of radiated energy losses, not included explicitly in the model depicted in Fig. 3.4.3*a*) be non-negative.

The first condition is met if the final state lies on or below, on a rigid unloading branch, the τ versus δ relation in a manner that is consistent with eq. (3.4.1). This shows that the final state lies on the spring unloading line at or beyond point B of Fig. 3.4.3*d*. The second condition requires that the final state satisfy

$$\tfrac{1}{2}(\tau_A+\tau)(\delta-\delta_A) \geqslant \int_{\delta_A}^{\delta} \hat{\tau}(\delta')\mathrm{d}\delta' \tag{3.4.3}$$

where $\tau = \hat{\tau}(\delta)$ denotes the τ versus δ relation for continued slip, τ and δ denote the final state, and subscript A denotes that at instability. Evidently, equality puts an upper limit on the final slip. The condition at that upper limit, denoted by E in Fig. 3.4.3*d*, is chosen so that the area under the straight line AE equals that under the curve $\tau = \hat{\tau}(\delta)$ between δ_A and δ_B. Of course, there may exist systems for which a construction like that in Fig. 3.4.3*c* applies at least approximately up to instability, but for which the same quasi-static τ versus δ relation becomes an inadequate model during the dynamic instability. Such would seem to be the case in the typical applications in references cited above of the stiffness based instability concept to faulting in deformation weakening systems, not just because of rate effects but because the dynamic development of slip may be kinematically different from the quasi-static development especially in large systems where slip regions spread at speeds near limiting wave speeds. Such systems cannot be described accurately as single degree of freedom systems.

The opposite limit from essentially uniform slip is illustrated with reference to Fig. 3.4.4. There the slipping region ($x_1 < 0$) is shown advancing into a portion of the fault that has not yet slipped ($x_1 > 0$), and the shear stress σ_{21} and slip Δu_1 are plotted schematically. These are related

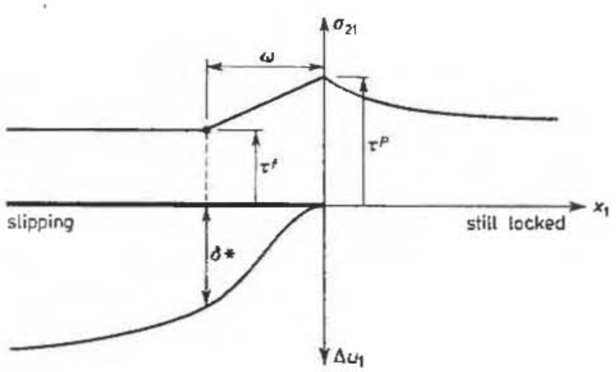

Fig. 3.4.4. Slip-weakening fault model, with zone ω of strength degradation confined to region near the advancing fault tip; see Fig. 3.4.2*a* for significance of τ^p, τ^f and δ_*.

to one another by $\sigma_{21} = \hat{\tau}(\Delta u_1)$ in the slipping region, and an application of eq. (3.2.53), recognizing that there is now no singularity at the crack tip, i.e.,

$$J_Q + \int_{(x_1)_Q}^{0} \sigma_{21} \frac{\partial \Delta u_1}{\partial x_1} \mathrm{d}x_1 = 0 \tag{3.4.4}$$

(refer to Fig. 3.2.3), shows that

$$J_Q - \tau^f (\Delta u_1)_Q = \int_0^{\delta *} [\hat{\tau}(\delta) - \tau^f] \mathrm{d}\delta \tag{3.4.5}$$

when point Q is chosen sufficiently far from the front of the slipping zone that the stress σ_{21} has reduced to the residual friction value τ^f. Here Δu_1 has been replaced by δ and it is recalled that $\delta *$ is the slip at which $\hat{\tau}(\delta)$ has decreased to τ^f, Fig. 3.4.2*a*.

The quantity $J_Q - \tau^f (\Delta u_1)_Q$ is invariant to the location of point Q so long as it is chosen sufficiently far from the front of the slipping zone that $\sigma_{21} = \tau^f$. When the linear extent ω of the zone of strength degradation in Fig. 3.4.4 occupies only a small fraction of the overall size of the slipping region, the invariant quantity can be evaluated from the elastic-brittle crack solution, formulated for the problem in which uniform resistive stress τ^f acts everywhere on the fault up to the tip. That problem has the conventional mode II elastic singularity, and if its associated energy release rate is denoted by G, then another application of eq. (3.2.53), valid under the presumption that $\omega \ll$ overall fault size, shows that

$$J_Q - \tau^f (\Delta u_1)_Q = G \tag{3.4.6}$$

Hence, by comparison to eq. (3.4.5), the critical G of elastic crack mechanics is shown to have the interpretation, from slip-weakening concepts,

$$G = \int_0^{\delta *} [\hat{\tau}(\delta) - \tau^f] \mathrm{d}\delta \tag{3.4.7}$$

This shows that in the limit considered, for which the linear extent ω of the zone of strength degradation is small, the predictions of slip-weakening fault models coincide with those of elastic-brittle crack mechanics with G defined as above (Ida, 1972; Palmer and Rice, 1973); see also Rice (1980) for further details. It should be emphasized that the above expression for G assumes ideally elastic behaviour of the surrounding material; inelastic response there provides another source for energy dissipation in the fracture process. Yamashita (1980) discusses slip-weakening crack growth with a linear viscoelastic model for the surroundings.

Palmer and Rice (1973) discuss estimates of the size ω of the zone of strength degradation. This actually depends on the detailed form of the τ versus δ relation, but not strongly so, and an approximate estimate is given by (Rice, 1980, eq. (6.12))

$$\omega_0 = [9\pi/16(1-\nu)]\mu\bar{\delta}/(\tau^p - \tau^f) \tag{3.4.8}$$

for mode II; the $(1-\nu)$ is deleted for mode III. Here $\bar{\delta}$ is a representative slip in the weakening process, defined by

$$\bar{\delta} = [1/(\tau^p - \tau^f)] \int_0^{\delta*} [\hat{\tau}(\delta) - \tau^f] \mathrm{d}\delta \tag{3.4.9}$$

Rice (1980) and Wong (1982) discuss various estimates of G and ω_0 based on τ versus δ relations inferred from laboratory data (on small specimens with nearly uniform slip) and on possible extrapolations to the tectonic scale. Values for G ranging from 5×10^3 to 5×10^4 $\mathrm{J \cdot m^{-2}}$ and for ω_0 of order 1 m are generally consistent with laboratory data. However, as discussed by Li and Rice (1983), the effective G values of order 5×10^6 $\mathrm{J \cdot m^{-2}}$ inferred indirectly from large scale earthquake instability models, and probably due to fault segmentation at some scale, imply sizes ω_0 that are of order 100 to 200 m if the strength drop $\tau^p - \tau^f$ is chosen as 50 MPa, and scales inversely with $(\tau^p - \tau^f)^2$ for a given G.

Interactions between pore fluids in surrounding rock and the spread of slip zones along faults can be analysed with the aid of the slip-weakening failure model and pore pressure effects on strength as in Fig. 3.4.2*b*. Rice (1979, 1980) gives a review of these mechanisms. The effect of those discussed is to stabilize somewhat the quasi-static spread of a slip zone against dynamic instability. However, processes or mechanisms which produce increased pore pressure on the fault plane, such as rapid dehydration, would have an opposite effect.

One effect of dynamic spread of a slip zone, at least under conditions for which the linear extent ω of the strength degradation zone is small, is to shorten ω from its value for quasi-static conditions. Thus, if ω_0 above represents the quasi-static value, then in steady dynamic spread of the slip zone (Rice, 1980, eq. (6.16))

$$\omega = \omega_0/f_{\mathrm{II}}(v), \quad \omega = \omega_0/f_{\mathrm{III}}(v) \tag{3.4.10}$$

for modes II and III, respectively, where the functions $f(v)$ are those defined by eq. (3.2.63). This effect may be of significance for the configurational stability of a single rupture plane; $\delta*/\omega$ represents an average displacement gradient of type $\partial u_1/\partial x_1$ (mode II) or $\partial u_3/\partial x_1$ (mode III) over the zone of strength degradation, and induces stresses (of type σ_{11} or σ_{13}) which are conducive to rupture on planes other than the main rupture plane. Thus, denoting $\langle\sigma_{11}\rangle$ and $\langle\sigma_{31}\rangle$ as averages of stress components along the slip surface over the region ω of strength degradation, and estimating $\delta_* = (9/4)\bar{\delta}$, Rice (1980, eqs. (6.17), (6.18)) shows that

$$\langle\sigma_{11}\rangle = \sigma_{11}^0 \pm \frac{4}{\pi}(\tau^p - \tau^f) f_{II}(v) \tag{3.4.11}$$

for mode II and

$$\langle\sigma_{13}\rangle = \sigma_{13}^0 \pm \frac{2}{\pi}(\tau^p - \tau^f) f_{III}(v) \tag{3.4.12}$$

for mode III. Here σ_{11}^0 and σ_{13}^0 are initial stresses acting before arrival of the slipping zone and the alternating signs refer to upper and lower surfaces of the zones. Since both f_{II} and f_{III} become unbounded as the respective limiting speeds are approached, these results show that stress alterations motivating fracture on directions off the main rupture plane become indefinitely large compared to those associated with the main plane itself. Some of the strongly segmented structure of actual faults may be due to effects of this type.

A related issue is that of when shear faults can exist as such. As is well known (e.g. Lawn and Wilshaw, 1975) laboratory attempts to simulate mode II or III ruptures generally result in local tensile cracking at crack tips in brittle solids. The above condition suggests, for example, that such tensile configurational destabilization of a mode II shear crack will not occur if (in quasi-static conditions) the initial stress σ_{11}^0 is sufficiently small or negative to ensure that

$$\sigma_{11}^0 + \frac{4}{\pi}(\tau^p - \tau^f) \leqslant \sigma_T \tag{3.4.13}$$

where σ_T, possibly zero, is the tensile strength of the faulted material.

Our discussion of the slip-weakening model in this sub-section has presumed unidirectional slip. Day (1982b) proposes a method for dealing with general slip paths as encountered in 3-*D* numerical fault dynamics. His method is consistent with isotropic hardening notions in continuum plasticity theory and may be described as follows: We let $\tau = \hat{\tau}(\delta)$ represent the unidirectional slip relation where now the interpretations $\tau = (\sigma_{21}^2 + \sigma_{23}^2)^{1/2}$ and

$$\delta = \int_0^t [(\Delta\dot{u}_1)^2 + (\Delta\dot{u}_3)^2]^{1/2}\, dt \tag{3.4.14}$$

are made and slip increments are distributed among the components according to

$$\Delta \dot{u}_1 = \dot{\delta}\sigma_{21}/\tau, \quad \Delta \dot{u}_3 = \dot{\delta}\sigma_{23}/\tau \tag{3.4.15}$$

3.4.2 Constitutive description of rate and state dependent frictional slip; instability conditions

A promising area of fault mechanics, not yet well developed, attempts to incorporate the actual rate and state dependences of the frictional slip process as observed experimentally into the theoretical framework for instability. In fact, almost all progress as of this writing has been on formulating appropriate constitutive relations and exploring their consequences for instability in the simplest context of the spring-slider system in Fig. 3.4.3*a*. Thus we give here only a brief report on this evolving area.

One characteristic of a constitutive relation intended for description of sequences of instabilities on the same fault surface is that there can be no fundamental dependence of stress on displacement. The dependence of this type postulated in slip-weakening models is plainly intended to model a single instability sequence. More generally it can be postulated that the strength $\tau(t)$ on a surface undergoing unidirectional slip of amount $\delta(t)$ is a direct function of slip velocity $V(t)$ [$= \mathrm{d}\delta(t)/\mathrm{d}t$] and (effective) normal stress $\sigma_n(t)$, and is a functional of the prior histories of both. Written symbolically

$$\tau(t) = F[V(t), \sigma_n(t); V(t'), \sigma_n(t'), -\infty < t' < t] \tag{3.4.16}$$

Recent experimental studies (Dieterich, 1978, 1979a, 1981; Ruina, 1980, 1983) have documented the velocity dependence in slip at fixed normal stress, $\sigma_n(t) =$ constant. These show the following features: When a step increase (decrease) in slip rate $V(t)$ is imposed, there results a step increase (decrease) in $\tau(t)$. That is, $\partial F[V(t), \ldots]/\partial V(t) > 0$. When slip at a constant rate $V(t)$ is maintained for some time, the stress $\tau(t)$ evolves towards a steady state value, denoted $\tau^{ss}(V)$, which is a function of V only (for the given σ_n) and which is independent of prior slip history. Further, it is often observed that $\mathrm{d}\tau^{ss}(V)/\mathrm{d}V < 0$, i.e. that the ultimate, or steady state, strength decreases with increasing velocity; exceptions seem to exist in the early stages of slip on a given surface and for slip at elevated temperature (Dieterich, 1981; Rice and Ruina, 1983; Ruina, 1983).

Ruina (1980, 1983), in further development of constitutive representations by Dieterich (1978, 1979a), related in turn to proposals by Rabinowicz

(1958), suggests that variables (say, $\theta_1, \theta_2, \ldots, \theta_n$) be introduced to describe the state of the slipping surface, that strength depends on V and the state as thus characterized, and that the state itself evolves with ongoing slip. Symbolically, this constitutive description has the form, for slip at fixed σ_n,

$$\tau = f(V, \theta_1, \ldots, \theta_n), \quad d\theta_i/dt = g_i(V, \theta_1, \ldots, \theta_n), \quad i = 1, \ldots, n \tag{3.4.17}$$

Thus the functions g_i describe the evolution of state during slip, and may possibly describe an evolution of state with time when the slip rate is zero. The equations $g_i = 0$, $i = 1, \ldots, n$, are presumed to have solutions $\theta_i = \theta_i^{ss}(V)$, which give the steady state appropriate to sustained slip at fixed speed V; the steady state strength is

$$\tau^{ss}(V) = f(V, \theta_1^{ss}(V), \ldots, \theta_n^{ss}(V)) \tag{3.4.18}$$

A specific two state variable form proposed by Ruina (1980, 1983) in order to fit results over a wide range of slip rates, approximately 0.01 to 1 $\mu m \cdot s^{-1}$, with polished quartzite surfaces is

$$\begin{aligned} \tau &= \tau_* + A\ln(V/V_*) + B_1\theta_1 + B_2\theta_2 \\ d\theta_{1,2}/dt &= -(V/L_{1,2})[\theta_{1,2} + \ln(V/V_*)] \end{aligned} \tag{3.4.19}$$

where all of θ_*, A, B_1, B_2, V_*, L_1 and L_2 are positive constants. For example, to fit experiments with the quartzite under $\sigma_n = 10$ MPa, the parameter choices are $\tau_*/\sigma_n = 0.55$ when V_* is chosen as 1 $\mu m \cdot s^{-1}$, $A/\sigma_n = 0.011$, $B_1/A = 1.00$, $B_2/A = 0.84$, $L_1 = 0.25$ μm, $L_2 = 5.2$ μm. As Gu *et al.* (1984) comment, the same form seems to describe qualitatively experiments with various gouge layers (Dieterich, 1981), except that the L's can be much larger, e.g. of the order of 100 μm. The steady state stress is

$$\tau = \tau_* - (B_1 + B_2 - A)\ln(V/V_*) \tag{3.4.20}$$

and for $B_1 + B_2 > A$ as above, this predicts velocity weakening in steady state slip.

A simpler but related mathematical form, employed by Ruina (1980, 1983) and Gu *et al.* (1984) in various stability analyses, and motivated originally as a simplification of a friction law proposed by Dieterich (1972a, 1981), involves a single state variable θ and is

$$\tau = \tau_* + A\ln(V/V_*) + B\theta, \quad d\theta/dt = -(V/L)[\theta + \ln(V/V_*)] \tag{3.4.21}$$

This is the form to which the two state variable law above reduces when $L_1 = L_2$ $(= L)$, if we define $B = B_1 + B_2$. In this case

$$\tau^{ss}(V) = \tau_* - (B - A)\ln(V/V_*) \tag{3.4.22}$$

Primary experimental features fitted by such laws are approximately logarithmic variations of strength with velocity, with positive coefficient (A) in instantaneous and negative (B_1+B_2-A) in long term (steady state) response, and approximately exponential decay of τ towards steady state with characteristic slip distances (the L's) that are independent of slip rate. In typical experiments of Dieterich and Ruina, slip is occurring in steady state at speed V_1 and the speed is suddenly changed to V_2. The general response found is illustrated schematically in Fig. 3.4.5.

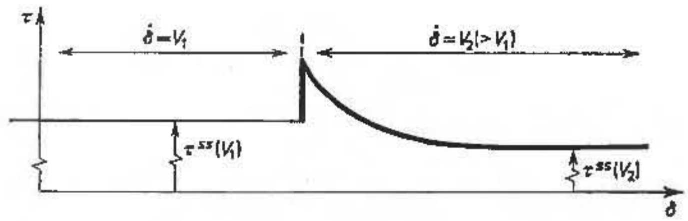

Fig. 3.4.5. Shear stress τ versus slip δ, with increase in slip rate $\dot{\delta}$ from V_1 to V_2; $\tau^{ss}(V)$ denotes the steady response for slip at rate V.

As remarked, most stability results so far obtained apply to the spring-slider system of Fig. 3.4.3*a*. Rice and Ruina (1983) examine the stability of steady state slip, enforced by imposed steady motion of the load point ($\mathrm{d}\delta_0/\mathrm{d}t = \text{const} = V_0$), in response to small perturbations and show within linearized theory that such slip changes from stable to unstable as the spring stiffness k is reduced below a critical value, k_{cr}, expressed by them in terms of parameters of the constitutive law. Further, the linearized response at $k = k_{cr}$ is oscillatory, and such oscillations decay or grow in time according to whether $k > k_{cr}$ or $k < k_{cr}$, respectively. For example, with the one state variable law of eqs. (3.4.21) above it is found that the critical stiffness is

$$k_{cr} = [(B-A)/L](1+mV^2/AL) \tag{3.4.23}$$

where m is the mass of the slider per unit base area, and the circular frequency of the oscillatory response at $k = k_{cr}$ is

$$\omega = (V/L)\sqrt{(B-A)/A} \tag{3.4.24}$$

An extended study of the quasi-static ($m = 0$) motions of the spring slider system with full inclusion of non-linearity (Gu *et al.*, 1984) for the one state variable law of eq. (3.4.21) shows that finite amplitude periodic oscillations of V about the imposed load point speed V_0 are found at $k = k_{cr}$ provided that the motion starts sufficiently close to the point in state space corresponding to steady state slip. All motions with $k < k_{cr}$ are unstable in that $V \to \infty$ in finite time (because inertia is here neglected). Motions with $k > k_{cr}$ are stable, in that $V \to V_0$ with increasing time, provided again that these begin sufficiently close to steady state. Sufficiently large disturbances induce instability ($V \to \infty$ in finite time) even when $k > k_{cr}$; however, the magnitude of the necessary disturbance, e.g. in the form of a suddenly increased imposed load point velocity on a system initially in steady state, is found to increase exponentially with k at large k.

Similar results are found by Gu *et al.* (1984) for the two state variable law, except that now stable limit cycle oscillations of V about V_0 are found over a small range of k values just below k_{cr}. These limit cycle motions are attractors for all states starting sufficiently near to steady state slip with k in that range; those states starting further away become unstable.

Special and explicit solutions are found by Gu *et al.* (1984) for the one state variable law when the load point is stationary, $V_0 = 0$. This may, among other possibilities, correspond to a case in which the load point is suddenly displaced and then held fixed; τ is then expressed as in eq. (3.4.2) where τ_0 is a given constant, representing the intensity of the suddenly applied loading. Such loading could, for example, simulate aftershock inducing stress transmission to fault segments in the vicinity of an earthquake rupture. The situation envisioned could also represent a fault segment which is loaded by ongoing tectonic processes, but at a sufficiently slow rate by comparison to kV (where V is the fault slip rate) that, for practical purposes, τ_0 in eq. (3.4.2) is constant. It is then found that all systems brought to a state of stress and slip velocity such that

$$\tau > \tau^{ss}(V)+kLB/(B-A) \tag{3.4.25}$$

are unstable, in that V accelerates continuously and $V \to \infty$ in finite time, the time being shorter the more the equality is violated. Here $\tau^{ss}(V)$ is given by eq. (3.4.22). All systems brought to a state of τ and V for which τ is less than the right-hand side of eq. (3.4.25) are stable in that, ultimately, V diminishes towards zero, although those brought to states with

$$\tau^{ss}(V)+kL < \tau < \tau^{ss}(V)+kLB/(B-A) \tag{3.4.26}$$

will first exhibit an increase in slip rate and only later a decrease.

Figure 3.4.6 shows the response to a more complicated load point motion. A system slides in steady state at speed V_0, the imposed load point speed. Then the load point motion is stopped for some relaxation time t_r, after which motion is resumed again at the same speed V_0. For the case illustrated, $B = 2A$ and the stiffness $k = 2k_{cr}$ where now $k_{cr} = A/L$. Gu *et al.* (1984) find that a critical relaxation time $t_r = 32L/V_0$ divides the unstable and stable range in this case, shorter times giving stability as illustrated. Similar analyses of effects of temporary relaxation of load point motion were made by Dieterich (1981) and Ruina (1983). The latter showed that peak stresses as predicted from the two state variable model of eqs. (3.4.19), with parameters chosen to fit velocity jump experiments on polished quartzite, gave a close fit to previous experimental results by Dieterich that had been interpreted as strengthening in stationary contact.

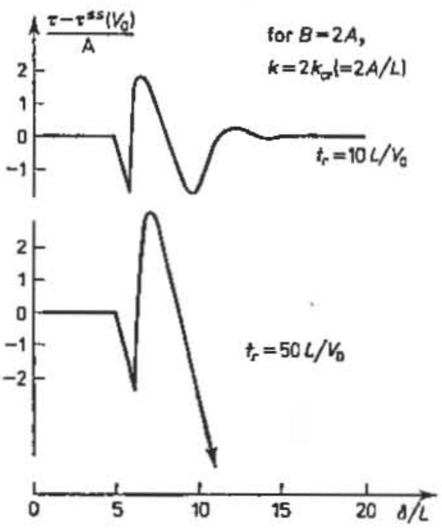

Fig. 3.4.6. Friction slip initially in steady state at speed V_0, then load point motion stopped for time t_r, then load point motion resumed at speed V_0.

In fact, the constitutive model as presented does not predict strengthening in truly stationary contact, and it is the fact that continuing relaxational slip occurs, albeit at very slow rates, which leads to the evolution of state manifested in sharp strength peaks (i.e. apparent strengthening) in Fig. 3.4.6.

The cases discussed thus far and also those treated elsewhere in the literature (Dieterich, 1979b, 1980, 1981; Mavko, 1980) show that the newly developed constitutive framework exhibits response that models key elements of the shear rupture process. For example, the calculations reported in Fig. 3.4.6 and other works referenced show that the constitutive relations can exhibit rapidly decaying strength with ongoing slip, a prerequisite for fracture instability, and can also exhibit effective regaining of a strength threshold necessary for future instabilities on the same surface. Also, the discussion in connection with inequality (3.4.25) suggests mechanisms of time-dependent failure for critically stressed systems, possibly related to aftershocks and to processes precursory to earthquake instability.

Some limited results for slip between deformable elastic continua (Ruina, 1980; Mavko, 1980; Rice and Ruina, 1983), rather than simply for single degree of freedom systems, suggest spatial propagations of slip events which seem in some correspondence to results observed on larger laboratory specimens (Dieterich, 1978, 1979b). In addition, direct measurement of stress versus slip histories, as crack-like confined slip events spread by measurement points in large sawcut laboratory specimens (Dieterich, 1980; Okubo and Dieterich, 1981; Lockner *et al.*, 1982), show τ versus δ relations resembling slip-weakening. This occurs on surfaces of a type which are known to exhibit frictional resistance described by constitutive laws of the general class discussed here, and suggests that there are connections yet to be drawn relating the new rate and state dependent constitutive framework to elastic-brittle crack mechanics and its slip-weakening extensions.

REFERENCES

Achenbach J. D. and Nuismer R. J. (1970), "Fracture generated by a dilatational wave", *Int. J. Fract. Mech.*, **1**, 77–88.

Achenbach J. D. and Abo-Zena A. M. (1973), "Analysis of the dynamics of strike-slip faulting", *J. Geophys. Res.*, **78**, No. 5, 866–875.

Aki K. (1968), "Seismic displacements near a fault", *J. Geophys. Res.*, **72**, 1217–1231.

Aki K. (1979), "Characterization of barriers on an earthquake fault", *J. Geophys. Res.*, **84**, 6140–6148.

Aki K. and Richards P. G. (1980), *Quantitative Seismology*, W. H. Freeman, San Francisco.

Andrews D. J. (1976), "Rupture velocity of plane-strain shear cracks", *J. Geophys. Res.*, **81**, 5679–5687.

Archuleta R. J. and Brune J. N. (1975), "Surface strong motion associated with a stick-slip event in a foam rubber model of earthquakes", *Bull. Seismol. Soc. Am.*, **65**, 1059–1071.

Archuleta R. J. and Frazier G. A. (1978), "Three-dimensional numerical simulations of dynamic faulting in a half-space", *Bull. Seismol. Soc. Am.*, **68**, 573–598.

Archuleta R. J. and Day S. M. (1980), "Dynamic rupture in a layered medium: The 1966 Parkfield earthquake", *Bull. Seismol. Soc. Am.*, **70**, 671–688.

Atkinson C. (1967), "A simple model of a relaxed expanding crack", *Archiv für Physik*, **33**, 38.

Atkinson C. and Eshelby J. D. (1968), "The flow of energy into the tip of a moving crack", *Int. J. Fract. Mech.*, **4**, 3.

Baker B. R. (1962), "Dynamic stresses created by a moving crack", *J. Appl. Mech.*, **29**, 449.

Barenblatt G. I., Salganik R. L. and Cherepanov G. P. (1962), "On the non-steady motion of cracks" (in Russian), *Applied Mathematics and Mechanics*, **26**, 469.

Berg C. A. (1968), "Relation between stress drop, fault friction, and crustal strength in shallow focus strike-slip faulting", *J. Geophys. Res.*, **73**, 2217.

Ben-Menahem A. (1961), "Radiation of seismic surface waves from finite moving sources", *Bull. Seismol. Soc. Am.*, **51**, 401–435.

Bilby B. A. and Eshelby J. D. (1968), "Dislocations and the theory of fracture", in: *Fracture, an Advanced Treatise*, H. Liebowitz (ed.), Vol. I, pp. 99–182, New York, N.Y.

Bouchon M. (1977), "San Fernando earthquake of 1971: Crack or dislocation" (abstract), *EOS Trans. AGU*, 58, 445.

Broberg K. B. (1960), "The propagation of a brittle crack", *Archiv für Physik*, Band 18, No. 10, 159–192.

Budiansky B. and O'Connell R. J. (1976), "Elastic moduli of a cracked solid", *Int. J. Solids and Structures*, **12**, 81–97.

Budiansky B. and Rice J. R. (1978), "On the estimation of a crack fracture parameter by long-wavelength scattering", *J. Appl. Mech.*, **45**, No. 2, 453–454.

Budiansky B. and Rice J. R. (1979), "An integral equation for dynamic elastic response of an isolated 3-D crack", *Wave Motion*, **1**, 187–192.

Burridge R. (1968), "Theoretical seismic sources and propagating brittle cracks", *J. Phys. Earth*, **16**, 83–92.

Burridge R. (1969), "The numerical solution of certain integral equations with nonintegrable kernels arising in the theory of crack propagation and elastic wave diffraction", *Philos. Trans. R. Soc. Lond.* **A 265**, 353–381.

Burridge R. and Willis J. (1969), "The self-similar problem of the expanding elliptical crack in an anisotropic solid", *Proc. Cambridge Phil. Soc.*, **66**, 443–468.

Burridge R. and Halliday G. S. (1971), "Dynamic shear cracks with friction as models for shallow focus earthquakes", *Geophys. J. R. Astron. Soc.*, **25**, 261–283.

Burridge R., Conn G. and Freund L. B. (1979), "The stability of a rapid mode II shear crack with finite cohesive traction", *J. Geophys. Res.*, **84**, No. B5, 2210–2222.

Cherepanov G. P. (1968), "Cracks in Solids", *Int. J. Solids Struct.*, **4**, 811–831.

Cherepanov G. P. and Afanas'ev E. F. (1974), "Some dynamic problems of the theory of elasticity—A review", *Int. J. Engn. Science*, **12**, 665–690.

Cherepanov G. P. (1979), *Mechanics of Brittle Fracture*, translation by A. L. Peabody from 1974 Russian edition with supplements, edited by R. DeWit and W. C. Cooley, McGraw-Hill.

Cleary M. P. (1976), "Continuously distributed dislocation model for shear-bands in softening materials", *Int. J. Num. Meth. Eng.*, **10**, 679–702.

Craggs J. W. (1960), "On the propagation of a crack in an elastic-brittle solid", *J. Mech. Phys. Solids*, **8**, 66.

Craggs J. W. (1966), "The growth of a disc-shaped crack", *Int. J. Engn. Sci.*, **4**, 113–124.

Das S. (1976), "A numerical study of rupture propagation and earthquake source mechanisms", Sc. D. Thesis, Massachusetts Institute of Technology.

Das S. and Aki K. (1977a), "A numerical study of two-dimensional spontaneous rupture propagation", *Geophys. J. R. Astron. Soc.*, **50**, 643–668.

Das S. and Aki K. (1977b), "Fault plane with barriers: A versatile earthquake model", *J. Geophys. Res.*, **82**, 5658–5670.

Das S. (1980), "A numerical method for determination of source time functions for general three-dimensional rupture propagation", *Geophys. J. R. Astron. Soc.* **62**, 591–604.

Das S. (1981), "Three-dimensional spontaneous rupture propagation and implications for the earthquake source mechanisms", *Geophys. J. R. Astron. Soc.*, **67**, 375–393.

Day S. M. (1979), "Three-dimensional finite difference simulation of fault dynamics", Final Report SSS-R-80-4295, Systems, Science and Software, La Jolla, California.

Day S. M. (1982a), "Three-dimensional finite difference simulation of fault dynamics: Rectangular faults with fixed rupture velocity", *Bull. Seismol. Soc. Am.*, **72**, No .3.

Day S. M. (1982b), "Three-dimensional simulation of spontaneous rupture: The effect of non-uniform prestress", *Bull. Seismol. Soc. Am.*, **72**, No. 6, 1881–1902.

Dieterich J. H. (1978), "Time dependent friction and the mechanics of stick slip", *Pure Appl. Geophys.*, **116**, 790–806.

Dieterich J. H. (1979a), "Modelling of rock friction. I. Experimental results and constitutive equations", *J. Geophys. Res.*, **84**, 2161–2168.

Dieterich J. H. (1979b), "Modelling of rock friction. II. Simulation of preseismic slip", *J. Geophys. Res.*, **84**, 2164–2175.

Dieterich J. H. (1980), "Experimental and model study of fault constitutive properties", in: *Solid Earth Geophysics and Geotechnology*, S. Nemat-Nasser (ed.), Appl. Mech. Div., Vol. 42, Amer. Soc. Mech. Engrs., N.Y., 21–30.

Dieterich J. H. (1981), "Constitutive properties of faults with simulated gauge", in: *Mechanical Behavior of Crustal Rocks*, N. L. Carter, M. Friedman, J. M. Logan, and D. W. Stearns (eds.), Geophys. Monogr. Ser. No. 24, Amer. Geophys. Union, 103–120.

Dmowska R. (1983), "Mathematical crack theory as applied to seismology", in: *Structure and Evolution of the Earth's Interior: A Monograph*, Polish Scientific Publishers, Warsaw (in Polish), 310–356.

Dmowska R., Rybicki K. and Teisseyre R. (1972), "Focal mechanism in connection with energy storage before crack formation", *Tectonophysics*, **14**, No. 3/4, 309–318.

Dmowska R. and Kostrov B. V. (1973), "A shearing crack in a semi-space under plane strain conditions", *Archives of Mechanics*, **25**, No. 3, 421–440.

Eaton J. P. (1967), "The Parkfield–Cholame, California earthquakes of June–August, 1966, instrumental seismic studies", *U.S. Geolog. Survey Profess. Paper*, **579**, 57–65.

Erdogan F. and Gupta G. D. (1972), "On the numerical solution of singular integral equations", *Quart. Appl. Moth.*, 525–534.

Eshelby J. D. (1957), "The determination of the elastic field of an ellipsoidal inclusion and related problems", *Proc. Roy. Soc. London, Ser.* **A241**, 376–396.

Eshelby J. D. (1969), "The elastic field of a crack extending non-uniformly under general anti-plane loading", *J. Mech. Phys. Solids*, **17**, 177.

Fossum A. F. and Freund L. B. (1975), "Non-uniformly moving shear crack model of a shallow focus earthquake mechanism", *J. Geophys. Res.*, **80**, 3343–3347.

Freund L. B. (1972a), "Energy flux into the tip of an extending crack in an elastic solid", *J. Elasticity*, **2**, 341–349.

Freund L. B. (1972b), "Crack propagation in an elastic solid subject to general loading, I, Constant rate of extension, II, Non-uniform rate of extension", *J. Mech. Phys. Solids*, **20**, 129–140, 141–152.

Freund L. B. (1976), "The analysis of elastodynamic crack tip stress fields", in: *Mechanics Today*, Vol. 3, S. Nemat-Nasser (ed.), Pergamon, N.Y., pp. 55–91.

Gu J-c., Rice J. R., Ruina A. L. and Tse S. T. (1984), "Slip motion and stability of a single degree of freedom elastic system with rate and state dependent friction", *J. Mech. Phys. Solids*, **32**, 167–196.

Hamano Y. (1974), "Dependence of rupture time history on the heterogeneous distribution of stress and strength on the fault plane" (abstract), *EOS Trans. Am. Geophys. Un.*, **55**, 352.

Hanson M. E., Sanford A. R. and Shaffer R. J. (1974), "A source-function for a dynamic brittle unilateral shear fracture", *Geophys. J. R. Astron. Soc.*, **38**, 365–376.

Haskell N. (1964), "Total energy and energy spectral density of elastic wave radiation from propagating faults, 1", *Bull. Seismol. Soc. Am.*, **54**, 1811–1842.

Hoenig A. (1978), "The behavior of a flat elliptical crack in an anisotropic elastic body", *Int. J. Solids and Structures*, **14**, 925–934.

Husseini M. I., Jovanovich D. B., Randall M. J., and Freund L. B. (1975), "The fracture energy of earthquakes", *Geophys. J. R. Astron. Soc.*, **43**, 367–385.

Ida Y. (1972), "Cohesive force across the tip of a longitudinal shear crack and Griffith's specific surface energy", *J. Geophys. Res.*, **77**, 3796–3805.

Ida Y. (1973), "The maximum acceleration of seismic ground motion", *Bull. Seismol. Soc. Am.*, **63**, 959–968.

Irwin G. R. (1960), "Fracture mechanics", in: *Structural Mechanics*, J. N. Goodier and N. J. Hoff (ed.), Pergamon Press, N. Y., p. 557.

Irwin G. R. (1962), "Crack extension force for a part through crack in a plate", *Trans. ASME, J. Appl. Mech.*, **29**, 651–654.

Jaeger J. C. and Cook N. G. W. (1979), *Fundamentals of Rock Mechanics*, 3rd ed., Chapman and Hall.

Kanamori H. (1970a), "Synthesis of long-period surface waves and its application to earthquake source studies—Kurile Islands earthquakes of October 13, 1963", *J. Geophys. Res.*, **75**, 5011–5027.

Kanamori H. (1970b), "The Alaskan earthquake of 1964—Radiation of long-period surface waves and source mechanism", *J. Geophys. Res.*, **75**, 5029–5040.

Kanamori H. (1971), "Seismological evidence for a lithospheric normal faulting, The Sanriku earthquake of 1933", *Phys. Earth Planet. Inter.*, **4**, 289–300.

Kanamori H. (1972), "Determination of effective tectonic stress associated with earthquake faulting, The Tottori earthquake of 1943", *Phys. Earth Planet. Inter.*, **5**, 426–434.

Kanamori H. (1977), "The energy release in great earthquakes", *J. Geophys. Res.*, **82**, 2981–2987.

Kanamori H. and Stewart G. S. (1976), "The mechanism of the Guatemala earthquake of February 4, 1976, revealed by teleseismic surface-wave and body-wave analysis", *EOS Trans. AGU*, **57**, 950.

Kasahara K. (1955), "A short discussion on ripples in earthquake shocks: After-shocks of the Boso-oki earthquake", *Bull. Earthquake Res. Inst. Tokyo Univ.*, **33**, 631–640.

Kostrov B. V. (1964a), "The axisymmetric problem of propagation of a tension crack", *Appl. Math. Mech.*, **24**, No. 4, 793–803 (in Russian).

Kostrov B. V. (1964b), "Self-similar problems of propagation of shear cracks", *J. Appl. Math. Mech.*, **28**, 1077–1087 (in Russian).

Kostrov B. V. (1966), "Unsteady propagation of longitudinal shear cracks", *J. Appl. Math. Mech.*, **30**, 1241–1248 (in Russian).

Kostrov B. V. (1975), "On the crack propagation with variable velocity", *Int. J. Fracture*, **11**, No. 1, 47–56.

Kostrov B. V. and Nikitin L. V. (1970), "Some general problems of mechanics of brittle fracture", *Arch. Mech. Stos.*, **22**, 750.

Lawn B. R. and Wilshaw T. R. (1975), *Fracture of Brittle Solids*, Cambridge.
Li V. C. and Rice J. R. (1983), "Pre-seismic rupture progression and great earthquake instabilities at plate boundaries", *J. Geophys. Res.*, 88, 4231–4246.
Lockner D. A., Okubo P. G. and Dieterich J. H. (1982), "Containment of stick-slip failures on a simulated fault by pore fluid injection", *Geophys. Res. Letters*, **9**. No. 8, 801–804.
Madariaga R. (1976), "Dynamics of an expanding circular fault", *Bull. Seismol. Soc. Am.*, **66**, 639–666.
Madariaga R. (1979), "On the relation between seismic moment and stress drop in the presence of stress and strength heterogeneity", *J. Geophys. Res.*, **84**, No. B5, 2243–2250.
Mavko G. M. (1980), "Simulation of creep events and earthquakes on a spatially variable model" (abstract), *Trans. Amer. Geophys. Un., EOS*, **61**, No. 46, 1120.
Mikumo T. and Miyatake T. (1979), "Earthquake sequences on a frictional fault model with a non-uniform strength and relaxation times", *Geophys. J. R. Astron. Soc.*, **59**, 497–522.
Miyatake T. (1980), "Numerical simulations of earthquake source process by a three-dimensional crack model, Part I. Rupture process", *J. Phys. Earth*, **28**, 565–598.
Molnar P., Tucker B. E. and Brune J. N. (1973), "Corner frequencies of P and S waves and models of earthquake sources", *Bull. Seismol. Soc. Am.*, **63**, 2081–2104.
Muskhelishvili N. I. (1953), *Some Basic Problems in the Mathematical Theory of Elasticity*, translated by J. R. M. Radok, Noordhoff, Groningen.
Muskhelishvili N. I. (1953), *Singular Integral Equations*, translated by J. R. M. Radok, Noordhoff, Groningen.
Niazy A. (1975), "An exact solution of a finite, two-dimensional moving dislocation in an elastic half-space with application to the San Fernando earthquake of 1971", *Bull. Seismol. Soc. Am.*, **65**, 1797–1826.
Okubo P. G. and Dieterich J. H. (1981), "Fracture energy of stick-slip events in a large scale biaxial experiment", *Geophys. Res. Lett.*, **8**, No. 8, 887–890.
Palmer A. C. and Rice J. R. (1973), "The growth of slip surfaces in the progressive failure of overconsolidated clay slopes", *Proc. Roy. Soc. Lond.*, Ser. **A332**, 527.
Paris P. C. and Sih G. C. (1965), "Stress analysis of cracks", in: *Symposium on Fracture Toughness Testing and Its Applications*, Special Technical Publication, No. 381, pp. 30–83, ASTM, Philadelphia.
Rabinowicz E. (1958), "The intrinsic variables affecting the stick-slip process", *Proc. Phys. Soc.*, **71**, part 4, 668–675.
Rice J. R. (1968a), "Mathematical analysis in the mechanics of fracture", in: *Fracture: An Advanced Treatise*, Vol. **2**, H. Liebowitz (ed.), Academic Press, N.Y., pp. 191–311.
Rice J. R. (1968b), "A path independent integral and the approximate analysis of strain concentration by notches and cracks", *J. Appl. Mech.*, **35**, 379.
Rice J. R. (1979), "Theory of precursory processes in the inception of earthquake rupture", *Gerl. Beitr. Geophys.*, **88**, 91–127.
Rice J. R. (1980), "The mechanics of earthquake rupture", in: *Physics of the Earth's Interior* (Proceedings of the International School of Physics "Enrico Fermi", Course 78, 1979), A. M. Dziewonski and E. Boschi (eds.), Italian Physical Society, North-Holland Publ. Co., pp. 555–649.
Rice J. R. and Ruina A. L. (1983), "Stability of steady frictional slipping", *Trans. ASME, J. Appl. Mech.*, **50**, 343–349.

Richter C. F. (1958), *Elementary Seismology*, W. H. Freeman and Co., San Francisco.

Rudnicki J. W. (1977), "The inception of faulting in a rock mass with a weakened zone", *J. Geophys. Res.*, **82**, 844–854.

Rudnicki J. W. (1980), "Fracture mechanics applied to the Earth's crust", *Ann. Rev. Earth Planet Sci.*, **8**, 489–525.

Rudnicki J. W. and Kanamori H. (1981), "Effects of fault interaction on moment, stress drop, and strain energy release", *J. Geophys. Res.*, **86**, No. B3, 1785–1793.

Ruina A. L. (1980), "Friction laws and instabilities: A quasi-static analysis of some dry frictional behavior", Ph. D. Thesis, Brown University, Providence, RI, USA.

Ruina A. L. (1983), "Slip instability and state variable friction laws", *J. Geophys. Res.*, **88**, 10359–10370

Rulyov B. G. (1975), "The prognostic aspect of seismic waves generated at a double source", *Dokl. Acad. Nauk SSSR*, **221**, 42–44 (in Russian).

Sato T. and Hirasawa T. (1973), "Body wave spectra from propagating shear cracks", *J. Phys. Earth*, **21**, 415–431.

Segall P. and Pollard D. D. (1980), "Mechanics of discontinuous faults", *J. Geophys. Res.*, **85**, 4337–4350.

Shmuely M. and Alterman Z. S. (1973), "Crack propagation by finite differences", *J. Appl. Mech.*, **40**, 902–908.

Sih G. C. (ed.), *Mechanics of Fracture* [Vol. I: Methods of analysis and solution of crack problems, 1973; Vol. II: Three-dimensional crack problems, 1975], Noordhoff, Leyden.

Spottiswoode S. M. and McGarr A. (1975), "Source parameters of tremors in a deeplevel gold mine", *Bull. Seismol. Soc. Am.*, **65**, 93–112.

Stoneley R. (1937), "The Mongolian earthquake of 1931, August 10", *Brit. Ass. Seism.* 42nd Rep., 5–6.

Stuart W. D. (1979a), "Strain softening prior to two-dimensional strike-slip earthquakes", *J. Geophys. Res.*, **84**, No. B3, 1063–1070.

Stuart W. D. (1979b), "Strain-softening instability model for the San Fernando earthquake", *Science*, **203**, 907–910.

Stuart W. D. and Mavko G. M. (1979), "Earthquake instability on a strike-slip fault", *J. Geophys. Res.*, **84**, No. B5, 2153–2160.

Tada H., Paris P. C. and Irwin G. R. (1973), *The Stress Analysis of Cracks Handbook*, Del Research Corp., Hellertown, Pennsylvania.

Takeuchi H. and Kikuchi M. (1973), "A dynamical model of crack propagation", *J. Phys. Earth*, **21**, 27–37.

Tchalenko J. S. and Berberian M. (1975), "Dasht-e Bayaz fault, Iran: Earthquake and earlier related structures in bedrock", *Geol. Soc. Am. Bull.*, **86**, 703–709.

Trifunac M. and Brune J. N. (1970), "Complexity of energy release during the Imperial Valley, California, earthquake of 1940", *Bull. Seismol. Soc. Am.*, **60**, 137–160.

Tsai Y. B. and Patton H. (1972), *Near-field Small Earthquakes—Dislocation Motion*, Semi-annual Technical Report No. 1, Texas Instruments, Inc. (prep. for Air Force Office Sci. Res. Contract F44620-72-C-0073).

Usami T. (1956), "Seismometrical study of Boso-oki earthquake of November 26, 1953", *Quart. J. Seismology, Japan Meteor. Agency*, **21**, 3.

Virieux J. and Madariaga R. (1982), "Dynamic faulting studied by a finite difference method", *Bull. Seismol. Soc. Am.*, **72**, No. 2, 345–369.

Walsh J. B. (1968), "Mechanics of strike-slip faulting with friction", *J. Geophys. Res.*, **73**, 761–776.

Weaver J. (1977), "Three-dimensional crack analysis", *Int. J. Solids Struct.*, **13**, 321–330.

Wong T. F. (1982), "Shear fracture energy of Westerly granite from post-failure behavior", *J. Geophys. Res.*, **87**, No. B2, 990–1000.

Wu F. T. and Kanamori H. (1972), "Source mechanism of February 4, 1965, Rat Island earthquake", *J. Geophys. Res.*, **78**, 6082–6092.

Wyss M. and Brune J. N. (1967), "The Alaska earthquake of 28 March 1964: A complex multiple rupture", *Bull. Seismol. Soc. Am.*, **57**, 1017–1023.

Yamashita T. (1980), "Quasi-static crack extensions in an inhomogeneous viscoelastic medium—a possible mechanism for the occurrence of aseismic faulting", *J. Phys. Earth*, **28**, 309–326.

Yoffé E. H. (1951), "The moving Griffith crack", *Philos. Mag.*, **42**, 739.